TECHNISCHE UNIVERSITÄT MÜNCHEN

Lehrstuhl für Biomolekulare Sensoren

(Univ.-Prof. Dr. T. Misgeld)

Mitochondrial transport during axon loss in a model of motor neuron disease and at the developing neuromuscular junction

Miriam Susanne Andrea Julika Reuter

Vollständiger Abdruck der von der Fakultät für Medizin der Technischen Universität München zur Erlangung des akademischen Grades eines Doktors der Medizin genehmigten Dissertation.

Vorsitzender: Univ.-Prof. Dr. E. J. Rummeny

Prüfer der Dissertation:

1. Univ.-Prof. Dr. T. Misgeld
2. Univ.-Prof. Dr. A. Konnerth

Die Dissertation wurde am 07.11.2012 bei der Technischen Universität München eingereicht und durch die Fakultät für Medizin am 12.06.2013 angenommen.

Contents

Abbreviations

ALS	Amyotrophic lateral sclerosis
AMPA	α-amino-3-hydroxy-5-methyl-4-isoxazolepropionic acid
ATP	Adenosine triphosphate
BTX	α-bungarotoxin
Ca^{++}	Calcium ions
CFP	Cyan fluorescent protein
fALS	Familial amyotrophic lateral sclerosis
FAT	Fast axonal transport
i.p.	Intraperitoneally
KHC	Kinesin-1 heavy chain
MAPK	Mitogen-activated protein kinase
Min	Minute
Mito	Mitochondria
NaN_3	Sodium azide
NGF	Nerve growth factor
NMDA	N-methyl-D-aspartate
NMJ	Neuromuscular junction
PBS	Phosphate-buffered saline
PFA	Paraformaldehyde
P10, P20, …	Postnatal day 10, postnatal day 20, …
SAT	Slow axonal transport
SEM	Standard error of the mean
SOD1	Cu/Zn superoxide dismutase
SOD^{G37R}	SOD1 with a mutation glycine to arginine at position 37
SOD^{G85R}	SOD1 with a mutation glycine to arginine at position 85
SOD^{G93A}	SOD1 with a mutation glycine to alanine at position 93
SOD^{WT}	Wild-type SOD1
TS	Triangularis sterni muscle
Wld^{S}	Wallerian degeneration slow
wt	Wild-type
YFP	Yellow fluorescent protein

Introduction

Mechanisms of axon loss

Dismantling of synaptic connections and neuronal processes occurs in neurodegeneration and after trauma, but also during normal development of the nervous system. While the importance of such axon loss in development and disease is well recognized, the mechanisms that mediate it are incompletely understood. Probably axon loss is mediated by a range of different mechanisms. Two broad categories of axon loss can already be differentiated by morphological criteria: *(1) Fragmentation* of large axon segments that occurs for example after axonal transection (Wallerian degeneration), but also during long-range 'pruning' of developing axon tracts (e.g. of axons of layer V pyramidal neurons) (Cowan, Fawcett et al. 1984). *(2)* A *'die-back'*-like pattern of axon loss that can be observed in some neurodegenerative diseases (e.g. amyotrophic lateral sclerosis) and during local axon branch dismantling in development (e.g. at neuromuscular junctions).

(1) Fragmentation: Transection of an axon leads to degeneration of its distal part, a process named Wallerian degeneration (Luo and O'Leary 2005). Wallerian degeneration is characterized by an initial latent phase, followed by microtubule disruptions and sudden fragmentation of the distal axon portion (Coleman and Freeman 2010). Originally, this process was believed to simply result from distal depletion of factor(s) needed for keeping an axon intact. However, discovery of a spontaneous gene mutation in mice that substantially prolongs survival of the distal axon fragment (*Wallerian degeneration slow* (*Wld^S*) *gene*) (Coleman, Conforti et al. 1998) changed this view. The *Wld^S* mutation instead suggests that Wallerian degeneration is a regulated and active process (Luo and O'Leary 2005). Of interest here is the fact that overexpression of the *Wld^S* gene product also affects the disease course in some neurodegenerative disease models. For example, it delays axon degeneration in a mouse model of motor neuron disease (*pmn*/*pmn* mice) (Ferri, Sanes et al. 2003). In contrast, the *Wld^S* genotype does not alter the clinical course of 'classical' mouse models of amyotrophic lateral sclerosis (such as those induced by mutations in the superoxide dismutase gene), which exhibit a 'die-back' fashion of neurodegeneration (Vande Velde, Garcia et al. 2004). *Wld^S* expression in mice also does not influence developmental axon loss at the neuromuscular junction (NMJ) (Parson, Mackintosh et al. 1997). Still, developmental dendritic pruning in Drosophila resembles Wallerian degeneration as it occurs by similar abrupt fragmentation preceded by microtubule disruptions (Williams and Truman 2005). The molecular pathways involved in Wallerian degeneration have been extensively studied in a number of different

species. There is growing evidence that intra-axonal NAD^+ and Ca^{++} levels play crucial roles in cytoskeletal breakdown and subsequent axonal degradation and might be influenced by the *Wld*^{S} gene product (Wang, Medress et al. 2012).

(2) 'Die-back': In some neurodegenerative diseases, such as amyotrophic lateral sclerosis, and in local branch elimination during development, a pattern of axon dismantling distinct from fragmentation is observed: axonal 'die-back'. During 'die-back', the axon does not fragment evenly along its length, but degeneration starts at the distal tips and is preceded by characteristic signs of 'atrophy', such as caliber variations (Fischer, Culver et al. 2004). Despite being a fairly common pattern in neuropathology, relatively little is known about the mechanisms in this form of axon loss. As axonal degeneration is the step that actually separates a neuron from its target, it is most likely an important contributor to the progressive phenotype in die-back neurodegenerative diseases, and represents a potential therapeutic target (Coleman and Perry 2002, Fischer, Culver et al. 2004). Die-back can be interpreted as a phenomenon of the 'last meadow', where availability of a limited resource for survival is curtailed; resulting in a chronic 'undernourishment' of distal sites (Fischer, Culver et al. 2004). Organelles and proteins delivered by axonal transport are obvious candidates for such limited resources, which is why die-back is commonly seen as indicative of transport disruptions. Indeed, chronic exposure to cytostatic drugs or toxins that target the cytoskeleton, and hence tracks for transport, often result in die-back neuropathies (Guiheneuc, Ginet et al. 1980). At the developing neuromuscular junction, dismantling axon branches show signs of local atrophy, such as thinning and terminal swellings ('retraction bulbs') (Bernstein and Lichtman 1999). Taken together, several observations suggest the hypothesis that reduced axonal transport might mediate forms of axon loss that involve die-back. My thesis set out to test the hypothesis of disturbed axonal transport by using techniques that allowed measuring axonal transport in individual axons and axon branches in murine motor neuron disease models and during synapse development.

Axonal transport

The idea that axonal transport plays a central role in many forms of neuronal pathology is in part based on the unique architecture of nerve cells: Neurons are polarized cells of an extreme geometry with a small cell body supporting neurites (dendrites and an axon) that contain the vast majority of a neuron's cytoplasm. Particularly axons can extend over long distances, some exceeding one meter or more in humans. The majority of molecules, organelles and cellular constituents originate in the soma and need to be actively delivered to their destination. This

makes neurons particularly dependent on effective intracellular transport (Coleman and Freeman 2010). Indeed, mutations in genes associated with axonal transport cause human neurodegenerative diseases (Duncan and Goldstein 2006). At the same time, in amyotrophic lateral sclerosis and other human neurodegenerative diseases, including Charcot-Marie-Tooth, Alzheimer's, Parkinson's and Huntington's disease, disruption of axonal transport is suspected to be an early and perhaps causative event in the disease process (De Vos, Grierson et al. 2008).

Axonal transport is generally active (adenosine triphosphate (ATP)-consuming) (Vale, Schnapp et al. 1985), directed (antero- *vs.* retrograde) and classified according to speed (fast - 1 µm/s - *vs.* slow - 0.1-20 mm/d). It requires specific subcellular machinery, which includes *(1) cytoskeletal tracks* (particularly microtubules), *(2) motor proteins* (e.g. kinesins and dynein) and *(3) associated molecules* (e.g. microtubule-associated proteins or motor-to-cargo adapters). Both fast and slow transport is mediated by the same molecular machinery, with slower speed being due to prolonged pauses of cargoes between 'runs' of movements (De Vos, Grierson et al. 2008).

(1) Cytoskeleton: The neuronal cytoskeleton consists of neurofilaments, actin filaments and microtubules. Neurofilaments provide structural stabilization and regulate axon caliber, and thereby control the speed of action potential conduction along the axon. There is evidence that neurofilaments can affect the function and dynamics of actin filaments and microtubules (Julien and Mushynski 1998), but proof for a direct role in transport is limited. Actin filaments contribute to cell integrity by stabilizing the plasma membrane. In addition to their structural role, actin filaments are used by myosin motor proteins for short-distance transport of vesicles or organelles (Hollenbeck and Saxton 2005, Letourneau 2009). The most important mechanism to deliver organelles and molecules to their site of destination is microtubule-based transport. Microtubules are polarized proteins, with a faster growing plus-end, which in axons is mostly directed towards the synapse, and a slower growing minus-end facing the cell body.

(2) Motor proteins: Two important classes of motor proteins are associated with microtubules: kinesin and dynein. Members of the kinesin super-family mostly mediate transport towards the microtubular plus-end pointing distally (anterograde), while dynein moves towards the minus-end (retrograde transport) (De Vos, Grierson et al. 2008). 45 members of the kinesin super-family have been identified in humans, some of which regulate microtubule dynamics rather than transport (Miki, Setou et al. 2001). Dynein requires for its function the formation of a co-complex with dynactin. Disruption of this complex results in late-onset motor neuron degenerative disease (LaMonte, Wallace et al. 2002). Kinesin and

dynein are considered to influence each other, so that disruption of transport in one direction affects transport in the opposite direction. For example, blocking kinesin with monoclonal antibodies results in bidirectional transport inhibition (Brady, Pfister et al. 1990).

(3) Associated molecules: Microtubule-associated proteins, such as tau, also influence axonal motility. This can occur by inhibition of molecular motors (Dixit, Ross et al. 2008), binding to microtubule, which creates a 'road-block' (Dixit, Ross et al. 2008) or by destabilization of microtubules through phosphorylated forms of tau protein (Cowan, Bossing et al. 2010). Additionally, a growing family of adapter proteins is being characterized that mediate or modulate binding between the transported cargoes and their molecular motors. Other molecules mediate docking of cargoes to the cytoskeleton, once the translocation machinery has disengaged (Kang, Tian et al. 2008). It is worth noting that probably so far we only know a fraction of the entire molecular machinery that regulates the biophysics of organelle translocation in neurons. Especially the mechanisms that mediate the diversity in movement patterns of different organelles and the specificity of cargo-adaptor-track interaction have thus far only been superficially characterized.

Mitochondrial distribution in neurons

Mitochondria have important functions in ATP production (via the citric acid cycle and the electron transport chain), β-oxidation of fatty acids, Ca^{++} homeostasis and apoptosis. They are especially needed at sites with high energy and Ca^{++}- buffering demands. In neurons, mitochondria concentrate in the soma, at synapses and around nodes of Ranvier, where ion gradients need to be maintained (Hollenbeck and Saxton 2005). Energy demands of neurons change depending of their activity; and efficient ATP supply and Ca^{++}- buffering must occur locally rather than by slow diffusion (Goldstein, Wang et al. 2008). Thus, mitochondrial distribution must respond to local activity changes, and as a consequence, neurons appear particularly vulnerable to defects in mitochondrial transport. Mitochondria are transported in both directions within axons and dendrites, with a pool staying stationary in the soma and along the length of the axon. Approximately two thirds of moving mitochondria are transported in anterograde and one third is transported in retrograde direction (Misgeld, Kerschensteiner et al. 2007). The average transport velocity of mitochondria falls between fast and slow transport (~ 0.5µm/s) (Hollenbeck and Saxton 2005), which is due to intermittent cessation of movement interspersed by 'runs' of a speed that corresponds to the speed of the involved molecular motors (~ 0.8-0.9 µm/s) (Gazzola, Burckhardt et al. 2009).

As in all cases of axonally transported materials, mitochondria depend in their trafficking on the interplay of cytoskeletal tracks, molecular motors and adapter proteins:

(1) Cytoskeleton: In axons, mitochondria move along microtubules and actin filaments. For long distance movement, microtubules provide the most important cytoskeletal tracks. Still, there is evidence that neurons require both types of cytoskeletal filaments to coordinate transport of organelles. In the absence of microtubules mitochondria were not capable to enter axons. However, if microtubules were abolished after mitochondria had entered an axon, mitochondria continued to move bidirectionally albeit with an altered motility pattern. Average and maximum velocities were reduced, and the balance of anterograde to retrograde transport was shifted towards net retrograde transport (Morris and Hollenbeck 1995). In the absence of actin filaments, mitochondria moved bidirectionally with increased velocities. Based on this and other evidence, it has been proposed that actin filaments provide a localized transport system, which serves to cluster organelles or to move organelles that have become dissociated from microtubules (Morris and Hollenbeck 1995).

(2) Motor proteins: The primary motor for anterograde movement of mitochondria along microtubules is kinesin-1. There is evidence that additional motor proteins can be involved in the movement of mitochondria, yet they play a minor role (Goldstein, Wang et al. 2008). Regulation of axonal transport is suspected not to reside in the motor proteins themselves, but in adaptor and regulatory proteins that are specific for different cargoes (Goldstein, Wang et al. 2008). For example, kinesin-1 is responsible for transport of mitochondria and synaptic vesicles, but vesicles travel exclusively within axons, whereas mitochondria are transported within axons and dendrites. This argues for additional regulatory elements.

(3) Associated molecules: In Drosophila, the adaptor complex required for mitochondrial transport consists of three proteins: kinesin-1 heavy chain (KHC), Miro (a protein in the outer mitochondrial membrane) and milton (an adaptor protein that links KHC to Miro and thereby recruits the motor to the mitochondrial surface) (Goldstein, Wang et al. 2008). Whereas Kinesin-1 is normally a tetramer of two heavy and two light chains, milton appears to replace the kinesin light chain during mitochondrial transport, which as a result does not require the light chain. Miro is now believed to mediate the Ca^{++}- sensitivity of mitochondrial transport, as this complex can cause detachment of mitochondria from microtubules upon calcium binding (Wang and Schwarz 2009). Another adaptor protein that is important for mitochondrial trafficking is syntabulin. Knockdown of syntabulin expression or blocking its interaction with kinesin-1 impair anterograde axonal transport of mitochondria (Cai and Sheng 2009).

A fraction of mitochondria does not move, presumably due to 'docking' to microtubules or neurofilaments (Hirokawa 1982). Special anchor proteins are likely to play an important role in the distribution of such stationary mitochondria (Hollenbeck 1996). The protein syntaphilin is selectively present on stationary mitochondria. By simultaneously binding to the mitochondrial surface and microtubules it might provide such an anchor. As expected from this model, deletion of the *Syntaphilin* gene results in a higher proportion of motile mitochondria (Kang, Tian et al. 2008).

The distribution of mitochondria needs to match changing metabolic demands. There is evidence that mitochondria do not cluster uniformly, but that distribution and transport can be regulated locally. Several intracellular signals have been found to influence mitochondrial distribution and transport. One important function of mitochondria is their Ca^{++}- buffering capacity via channels and transporters in the mitochondrial membrane. Ca^{++} influx in neurons occurs at pre- and postsynaptic sites, where at the same time a lot of energy substrates are required to maintain ion gradients. Thus, it seems intuitive that elevated cytosolic Ca^{++} levels can arrest microtubule-based mitochondrial movement and thereby deposit them at sites where Ca^{++}- buffering and energy requirements are high. Ca^{++}- binding EF hands within the Miro protein are considered to mediate the detachment of mitochondria from microtubules (Goldstein, Wang et al. 2008, Wang and Schwarz 2009). Mitochondrial transport within axons is also modulated by electrical activity and myelination. At nodes of Ranvier (where energy demands would be expected to be higher than in internodes), mitochondrial speed is significantly reduced compared to internodal regions (Ohno, Kidd et al. 2011). Another type of movement regulation might be via O-GlcNAcylation of milton, as the enzyme activity of O-GlcNA transferase is dependent on glucose concentration in the cell (Goldstein, Wang et al. 2008, Murrey and Hsieh-Wilson 2008, Wang and Schwarz 2009). Thus, local glucose levels may bias mitochondrial movement towards sites with high supply of substrates (Goldstein, Wang et al. 2008). Neurotransmitters (serotonin and dopamine) were shown to influence mitochondrial motility through a signalling cascade that involves modulation of the Akt and glycogen synthase kinase (GSK3β) pathways (Chen, Owens et al. 2007, Chen, Owens et al. 2008). Activation of nerve growth factor (NGF) receptors has been shown to result in an accumulation of mitochondria via local increase in transport. This happens at least in part via the phosphatidylinositol-(3,4,5)-trisphosphate and mitogen-activated protein kinase (MAPK) signalling pathways. The targets of the kinases are not certain; they might act through phosphorylation of kinesin-1 (Chada and Hollenbeck 2003, Goldstein, Wang et al. 2008). It should be kept in mind, however, that many of these regulatory influences still need to be confirmed *in vivo* in fully matured vertebrate axons.

Amyotrophic lateral sclerosis

Definition and clinics

The term amyotrophic lateral sclerosis (ALS) is used to cover a spectrum of neurodegenerative syndromes characterized by progressive degeneration of motor neurons. It is a late-onset neurodegenerative disease of unknown etiology, which affects motor neurons in the primary motor cortex, brainstem and spinal cord. Generally, the disease leads to paralysis and death within 1-5 years after the first symptoms develop (Boillee, Vande Velde et al. 2006). Degeneration of anterior horn cells (lower motor neurons) results in atrophy and fasciculation of affected muscles. Spasticity can be observed in atrophic muscles, indicating additional death of upper motor neurons and loss of inhibitory input. Approximately two thirds of the patients have a spinal form of the disease with symptoms starting in the upper or lower limbs. In contrast, bulbar onset of the disease is characterized by dysarthria and dysphagia as the first symptoms. Sensory deficits in clinical examination are not typical in ALS, although some patients exhibit abnormalities in sensory nerve conduction studies (Pugdahl, Fuglsang-Frederiksen et al. 2007).

The diagnosis of ALS is based on clinical history, examination, electromyography, nerve conduction studies and exclusion of 'ALS mimics', such as cerebral lesions and tumours, multiple sclerosis, cervical spondylotic myelopathy, cervical disc prolaps, poliomyelitis, multifocal motor neuropathy, spinal muscular atrophy, Kennedy's disease and inclusion body myositis (Wijesekera and Leigh 2009). The pathological hallmarks of the disease were first described by the French neurologist Jean-Martin Charcot in 1869. Charcot observed a distinct 'myelin pallor' in the corticospinal tracts of two patients with progressive muscular atrophy, representing degeneration of upper motor axons and their replacement by gliosis (Boillee, Vande Velde et al. 2006). ALS is a 'die-back' neuropathy, meaning the nerve-muscle connection at the neuromuscular junction is lost before degeneration of the axon or death of the neuron (Fischer, Culver et al. 2004). As a transient compensatory mechanism, spared motor units sprout and transiently re-innervate vacated NMJs (Schaefer, Sanes et al. 2005). Accumulations of organelles and proteins are observed in somata and proximal motor axons of ALS patients - which could be cause or consequence of disturbed transport (Boillee, Vande Velde et al. 2006).

Extraocular muscles and sphincter muscles of the bowel are generally spared from denervation in ALS. Indeed, most patients have normal eye movements on clinical examinations. Still, some patients have difficulties in saccade generation, smooth pursuit movements and ocular fixation (Donaghy, Thurtell et al. 2011). Immunohistochemical analyses

of extraocular muscles from ALS patients show mostly well preserved cytoarchitecture with only mild alterations (like larger variations in muscle fiber size and altered myosin heavy chain content compared to control cases) (Ahmadi, Liu et al. 2010). This indicates that extraocular muscles are either not affected by motor axon degeneration or that neighbouring axons are competent in reinnervating denervated NMJs for longer periods, since extraocular motor units are smaller than in most other muscles (Ahmadi, Liu et al. 2010).

Epidemiology and genetics

The prevalence of ALS is reported to be 4-6 per 100,000 in western countries; the life-time risk has been estimated at 1 in 1,000 (Boillee, Vande Velde et al. 2006). The mean age of onset is between 50 and 60 years, with approximately 5% of the cases having an onset before the age of 30 years (Wijesekera and Leigh 2009). In most instances ALS occurs sporadically, but in approximately 10% of the cases several family members are affected (referred to as familial amyotrophic lateral sclerosis, fALS). ALS can be inherited in an autosomal-dominant, autosomal-recessive and X-linked manner. Patients with familial and sporadic ALS are clinically indistinguishable and show similar pathological hallmarks, including a die-back neuropathy, protein accumulations and mitochondrial alterations (Boillee, Vande Velde et al. 2006). However, some studies report that the age of onset in fALS is earlier than in the sporadic form of the disease (Wijesekera and Leigh 2009).

Some of the chromosomal loci containing mutations in fALS have been identified. Affected loci include genes encoding Cu/Zn superoxide dismutase (SOD1), TDP-43, angiogenin, vascular endothelial growth factor, vesicle associated protein B and neurofilament heavy-subunit (Boillee, Vande Velde et al. 2006, Rothstein 2009). Mutations in the Cu/Zn superoxide dismutase are responsible for approximately 20% of all fALS cases. SOD1 is a ubiquitously expressed, primarily cytosolic enzyme that converts superoxide radicals (which are by-products of the respiration chain) to hydrogen peroxide, thus playing a role in the anti-oxidant defence of cells (Bacman, Bradley et al. 2006). SOD1 contains copper and zinc as prosthetic groups, which are inserted into the enzyme aided by an SOD1-specific copper chaperone (copper chaperone of SOD1, CCS) (Bacman, Bradley et al. 2006). The first missense mutations in the *SOD1* gene were reported in 1993 (Rosen, Siddique et al. 1993). By now more than 110 mutations in all five exons, at intronic sites and the 3' untranslated region of the SOD1 gene are known, nearly all which are inherited in an autosomal-dominant manner (Boillee, Vande Velde et al. 2006). The effect of mutant SOD1 is considered to be an unknown gain of function toxicity, since deletion of the *SOD1* gene in mice does not lead to motor neuron pathology (Reaume, Elliott et al. 1996). Mice expressing mutant forms of human SOD1 develop

progressive motor neuron degeneration comparable to ALS (Gurney, Pu et al. 1994). Most of our knowledge about the mechanisms underlying motor neuron pathology in ALS derives from studies using transgenic mice that harbor numerous copies of mutant human *SOD1* in their genome (Boillee, Vande Velde et al. 2006). A variety of SOD1-mutant mouse lines have been generated, which differ in terms of pathogenic mutations and the genomic copy number of the transgene. Some lines express enzymatically active forms of SOD1 (e.g. SOD^{G93A}, SOD^{G37R}), while others express inactive forms of the protein (e.g. SOD^{G85R}). Those mouse lines differ phenotypically in terms of disease onset and progression.

Pathogenic mechanisms in ALS and SOD1-mutants

The etiology of neurodegeneration in amyotrophic lateral sclerosis is unknown. However, mostly based on studies in ALS patients or murine SOD1 models, a number of pathomechanistic hypotheses have been formulated. The selective vulnerability of motor neurons to degeneration might for instance be based on any combination of the following mechanisms:

(1) Intracellular aggregates: Aggregation of misfolded proteins (including SOD1 and neurofilaments) are suggested to contribute to motor neuron toxicity. Cytoplasmic protein aggregates could be detected in tissues from ALS patients and murine SOD1 models (Watanabe, Dykes-Hoberg et al. 2001). SOD1 protein aggregates were found selectively in motor neurons, but not in dorsal root ganglionic or hippocampal neurons (Durham, Roy et al. 1997).

(2) Mitochondrial dysfunction: Although SOD1 is localized primarily in the cytosol, a fraction of wild-type (wt) and misfolded mutant SOD1 was found to be localized within spinal cord mitochondria (Vande Velde, Miller et al. 2008). Histopathological studies showed alterations of mitochondrial morphology in anterior horn perikarya from both sporadic and familial ALS patients (Hirano, Donnenfeld et al. 1984, Hirano, Nakano et al. 1984, Sasaki and Iwata 2007). Such alterations were also found in some SOD1-mutant mouse models (SOD^{G93A}, SOD^{G37R}) and manifested as massive mitochondrial vacuolation and expansion of the intermembrane space (Higgins, Jung et al. 2003). Targeting mutant SOD1 to mitochondria was sufficient to induce neuronal toxicity in cell cultures and SOD^{G93A} mouse models (Magrane, Hervias et al. 2009, Igoudjil, Magrane et al. 2011) - suggesting that mitochondrial mislocalization of mutant SOD1 might directly initiate motor neuron degeneration. Biochemical dysfunction of the mitochondrial electron transport chain was reported from studies with human ALS patients,

animal models and in cell cultures (Boillee, Vande Velde et al. 2006). Recent studies suggested mitochondrial fusion defects in *SOD*^{G93A} primary motor neurons (Magrane, Sahawneh et al. 2012). However, the exact role of mitochondrial dysfunction in disease onset and progression remains uncertain (Bacman, Bradley et al. 2006).

(3) Apoptotic pathways: In terminal stages of ALS, motor neuron death involves the intrinsic mitochondria-dependent apoptotic pathway. Overexpression of the anti-apoptotic protein Bcl-2 delayed neurodegeneration in *SOD*^{G93A} mice (Azzouz, Hottinger et al. 2000). Both wild-type and mutant SOD1 directly bound Bcl-2 in mouse and human spinal cords, suggesting a direct link between SOD1 and the apoptotic pathway (Bacman, Bradley et al. 2006, Boillee, Vande Velde et al. 2006). Targeting mutant SOD1 to mitochondria in cell cultures led to release of mitochondrial cytochrom-c, activation of the caspase cascade and induction of cell death (Takeuchi, Kobayashi et al. 2002). At the same time, the fact that pathology within motor neurons is first seen at distal sites within the cells, argues against a primarily somatic cell death mechanism as initiating step of the pathogenic cascade.

(4) Reactive oxygen species: Mitochondrial respiration is the main source of reactive oxygen species (ROS) in the cell, and ROS levels tend to increase when respiration is impaired (Bacman, Bradley et al. 2006). The involvement of mitochondria and the enzyme SOD1 in ALS suggest that oxidative stress might play a role in the pathogenesis of the disease. Enhanced protein and lipid oxidation were found in spinal cord motor neurons and glial cells of patients with sporadic ALS (Shibata, Nagai et al. 2001). An elevation of ROS and oxidation of proteins, DNA and membrane phospholipids were also found in spinal cords of SOD1-mutant mice (Liu, Wen et al. 1999). ROS scavenging enzymes (including peroxiredoxin-2 and glutathione peroxidase-1) were shown to co-aggregate with SOD1, suggesting that SOD1 aggregates indirectly affect the cellular ROS-scavenging system (Kato, Saeki et al. 2004).

(5) Impaired Ca^{++} homeostasis: Increased intracellular Ca^{++} levels are implicated in necrosis and apoptosis (Bacman, Bradley et al. 2006) and were found in the *SOD*^{G93A} mouse model (Tradewell, Cooper et al. 2011). In motor neurons mitochondria are an important Ca^{++} buffer, as these cells lack additional Ca^{++}- buffering proteins, such as parvalbumin and calbindin D28K (Ince, Stout et al. 1993). Mitochondrial dysfunction could therefore lead to a pronounced vulnerability of motor neurons to impaired calcium homeostasis.

(6) Glutamate excitotoxicity: The excitatory neurotransmitter glutamate leads to an influx of Ca^{++} through N-methyl-D-aspartate (NMDA) and α-amino-3-hydroxy-5-methyl-4-isoxazolepropionic acid (AMPA) receptors. Increased glutamate levels in the cerebrospinal fluid

were found in approximately 40% of sporadic ALS patients and correlated with disease severity (Spreux-Varoquaux, Bensimon et al. 2002). Under physiological conditions, glutamate is removed rapidly from the synaptic cleft to prevent repetitive firing and excitotoxicity. The astrocytic glutamate transporter EAAT2 (excitatory amino acid transporter 2) has an important function in the removal of synaptic glutamate (Rothstein, Dykes-Hoberg et al. 1996). Decreased EAAT2 protein levels were observed in *SOD*^{G85R}-mutant animals (Bruijn, Becher et al. 1997). Mutant SOD1 was found to inactivate the transporter in the presence of hydrogen peroxide, suggesting that EAAT2 is a target of mutant SOD1 toxicity (Trotti, Rolfs et al. 1999). Accordingly, the glutamate antagonist riluzole can slow the progression and prolong life-span in ALS patients (Bensimon, Lacomblez et al. 1994).

(7) Glial cell pathology: Glial cells appear to contribute to the selective degeneration of motor neurons in ALS. Analyses of chimerical mice, with cells expressing mutant SOD1 interspersed in a wild-type micro-environment, revealed abnormalities and degeneration of wild-type motor neurons surrounded by mutant SOD1-expressing glial cells (Di Giorgio, Carrasco et al. 2007, Julien 2007). In ALS, astrocytes were shown to secrete so far unidentified factors that induce or exacerbate degeneration of motor neurons. Candidates are inflammatory signals, such as cytokines (e.g. TNF-α, interleukins) (Julien 2007, Nagai, Re et al. 2007). Microglial cells seemed to exert additional non-cell autonomous toxicity, which affects disease progression more than onset (Beers, Henkel et al. 2006). Importantly, expression of mutant SOD1 in motor neurons, microglial cells or astrocytes alone failed to induce motor neuron impairment (Gong, Parsadanian et al. 2000, Lino, Schneider et al. 2002, Boillee, Vande Velde et al. 2006). Finally, motor neuronal genotype appeared to influence vulnerability to exogenous damage (Di Giorgio, Carrasco et al. 2007, Julien 2007), suggesting a 'two-hit' model, where genetic and environmental stressors synergize to affect an intrinsically vulnerable neuronal population. A possibly pathogenic role of glial cells has to be considered in studies that differentiate induced pluripotent stem cells into motor neurons with the aim of autologous cell replacement therapies (Dimos, Rodolfa et al. 2008).

(8) Cytoskeletal abnormalities: One early pathological hallmark in motor axons of SOD1 mice is the accumulation of hyperphosphorylated neurofilaments (Hirano, Donnenfeld et al. 1984, Hirano, Nakano et al. 1984). Neurofilament content in axons was reduced at the onset of symptoms (Zhang, Tu et al. 1997). Variant alleles of the neurofilament heavy-subunit gene (*NF-H*) were found in human ALS patients (Collard, Cote et al. 1995). Transgenic mice expressing high levels of human NF-H develop a neuropathy characterized by muscle atrophy and generalized tremor, and serve as a model for ALS (Cote, Collard et al. 1993, Collard, Cote et al.

1995, Julien, Cote et al. 1995). Modulation of the neurofilament gene expression pattern, in form of deletion of neurofilaments or overexpression of the heavy chain, had a protective effect on motor neurons expressing mutant SOD1 (Couillard-Despres, Zhu et al. 1998, Williamson, Bruijn et al. 1998). Together, these results suggest that the intermediate filament network might at least modulate neurodegeneration in ALS.

(9) Disturbed axonal transport: Most relevant to my study is the hypothesis that disturbed axonal transport might be a direct mediator of motor neuron death in ALS. The 'die-back'-pattern with distal degeneration was suggested to represent size-dependent 'undernourishment' (Fischer, Culver et al. 2004). Axonal transport was found to be disturbed in ALS patients and mouse models of the disease (Collard, Cote et al. 1995, Sasaki and Iwata 1996, Zhang, Tu et al. 1997, Warita, Itoyama et al. 1999, Williamson and Cleveland 1999). Reduced transport rates occur early in the disease and both slow and fast axonal transport are affected. Mutant SOD1 was found to co-aggregate with dynein, suggesting a physical inhibition of dynein/dynactin function (Ligon, LaMonte et al. 2005). Other possible mechanisms how mutant SOD1 could cause transport deficits include disruption of microtubule formation/stability, interaction with motor proteins, inhibition of cargo-binding sites, mitochondrial damage and elevated intracellular Ca^{++} levels (De Vos, Grierson et al. 2008). Several studies predicted a cargo- and direction-specific disruption of transport (Sasaki and Iwata 1996, Warita, Itoyama et al. 1999, Williamson and Cleveland 1999, De Vos, Chapman et al. 2007, Bilsland, Sahai et al. 2010); however, so far no consensus has been reached regarding which components of the transport machinery are most affected, and which ones might be most relevant to pathogenesis. Hence, it remains unclear, whether transport deficits contribute to ALS pathogenesis and how they correlate with disease initiation or progression.

The first part of my thesis aimed at clarifying the relationship between organelle transport deficits and degenerative changes at the single neuron level in intact preparations (Part 1).

Synapse elimination in the postnatal development of the neuromuscular junction

Elimination of neuronal processes can be disease-causing, but is also part of normal development. Many regions of the developing nervous system undergo regressive events. These events involve loss of supernumerary neurons (Oppenheim 1991), as well as local elimination of axon branches and synaptic connections without loss of the parent neurons. This latter process is referred to as synapse elimination (Sanes and Lichtman 1999, Misgeld 2005). Synapse elimination is particularly well-studied at the neuromuscular junction (Sanes

and Lichtman 1999), the synapse of a motor axon terminal (presynaptic site, input) with the motor end plate of a muscle fiber (postsynaptic site).

In mature mammals each muscle fiber is innervated by exactly one motor axon branch. However, in early postnatal animals every postsynaptic site is contacted by multiple axon branches from different motor neurons. During the first two postnatal weeks (in mice) all except one branch are eliminated by undergoing a process called 'axosome-shedding' (Bishop, Misgeld et al. 2004). In contrast, the remaining axon branch enlarges its synaptic territory and is normally maintained throughout life (Sanes and Lichtman 1999).

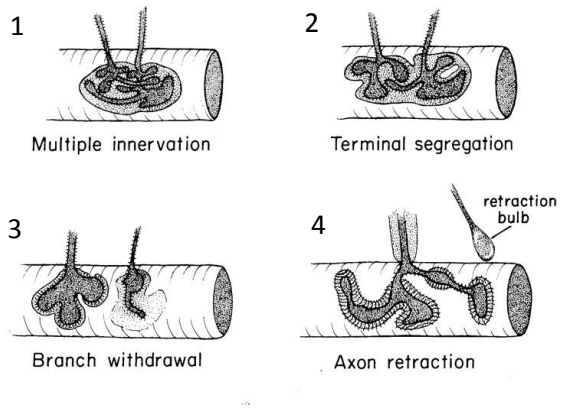

Figure 1: Transition from multiple- to single-innervation at postnatal neuromuscular junctions (from Sanes and Lichtman 1999)

The number of motor neurons innervating a muscle does not change during this phase of development, as all motor neurons withdraw only a subset of their branches (Sanes and Lichtman 1999). As a result motor units shrink, allowing for more precise and graded force generation (Wyatt and Balice-Gordon 2003). The process of synapse elimination is distinct from Wallerian degeneration and unaltered in *Wld*^{S} mice (Parson, Mackintosh et al. 1997). Before axons lose contact to the muscle fiber, they show morphologic signs of dystrophy, like local thinning and swellings. Retreating axons ('loser' branches) end in a swollen bulb (referred to as 'retraction bulb') (Riley 1981, Balice-Gordon, Chua et al. 1993); and at least a fraction of the axon branch's material is shed as membrane-enclosed 'axosomes'. These axosomes are enveloped by Schwann cells, suggesting an involvement of glial cells in the elimination process (Bishop, Misgeld et al. 2004). Increased lysosomal activity is associated with developmental synapse elimination, consistent with digestive mechanisms such as autophagy and heterophagy (Song, Misgeld et al. 2008). Whether there is also a fraction of axonal content that is retracted towards the persisting axon is not yet clear (Bishop, Misgeld et al. 2004). One model predicts the 'evacuation' of organelles from dismantling axon branches by loss of anterograde and/or increased retrograde transport (Riley 1981).

Since every muscle fiber ends up being innervated by exactly one motor axon branch ('winner' branch), the elimination of inputs must be a regulated rather than a random process (Wyatt and Balice-Gordon 2003). Relatively little is known about the factors that mediate competition between branches. One factor suspected to mediate competition is the degree of correlation in the spiking patterns of two inputs. Uncorrelated activity enhances competition, whereas correlated activity diminishes competition (Personius and Balice-Gordon 2001). The outcome is influenced by the relative level of activity between converging axons, suggesting that strong inputs are able to destabilize weaker inputs (Balice-Gordon and Lichtman 1994, Buffelli, Burgess et al. 2003). Such mechanisms would imply a hierarchy of neurons. One axon with the 'best' (i.e. most efficient) activity pattern would maintain all its branches and another axon with the 'worst' activity pattern would completely withdraw from the muscle (Kasthuri and Lichtman 2003). This outcome, however, has not been observed. Instead, each motor neuron wins part of its competitions while losing others (Keller-Peck, Walsh et al. 2001, Kasthuri and Lichtman 2003), indicating that there are factors that modulate 'competitiveness' (also known as 'competitive vigor'), as a motor pool progresses through competition. Winning one competition now would come at the expense of subsequently reduced vigor, dynamically changing the vigor hierarchy. One hypothesis claims that vigor depends on the local distribution of resources within an axon (Barber and Lichtman 1999). Consequently, neurons with larger arborizations would be at a disadvantage compared to neurons that have already pruned some of their branches (Kasthuri and Lichtman 2003). Distribution of a resource could be regulated locally via the amount of transport into branches. Reduced anterograde transport could lead to depletion of resources, like nutrients, neurotransmitters and organelles, and could thus promote elimination of the respective branch (Buffelli, Burgess et al. 2003). At the same time, other branches of the same neuron would benefit from the redistribution. Disparities (reductions or elevations) in retrograde transport could for example affect signalling molecules (e.g. neurotrophic or growth factors) and come as a competitive advantage or disadvantage for ongoing and upcoming competitions.

The second part of my thesis contains the exploration of transport changes selectively in dismantling branches - and hence tests the idea of evacuation of loser branches, as well as the possibility of axonal transport as a means of resource redistribution (Part 2).

Synapse elimination is considered to be a rather local event, whereas neurodegenerative diseases often affect several cellular subcompartments of neurons. Still, this discrepancy does not exclude common regulative, respectively pathogenic mechanisms. Many pathogenic events are considered to result from dysregulation of physiologically occurring processes.

Axonal transport could on the one hand be regulated locally during the elimination of individual axon branches. On the other hand reductions in axonal transport are a promising pathogenic event in many neurodegenerative diseases.

Aim of the thesis

Aim of this thesis was to investigate mitochondrial transport during axon loss in a mouse model of motor neuron disease and at the developing neuromuscular junction.

The first project aimed to investigate mitochondrial transport in motor axons from an established mouse model of amyotrophic lateral sclerosis. There is evidence from prior studies that axonal transport is reduced early in patients and mouse models with motor neuron disease. So far axonal transport measurements have been based on investigations of organelle densities (Pun, Santos et al. 2006, Vande Velde, McDonald et al. 2011), [^{35}S]methionine-containing proteins after spinal cord injections (Williamson and Cleveland 1999) and in vitro organelle tracking (De Vos, Chapman et al. 2007, Magrane, Sahawneh et al. 2012). Those methods did not provide an opportunity to directly observe transport in motor axons within their natural environment. A recent study using in vivo imaging, which was published after initiation of my project, yielded inconclusive results with regards to mitochondrial transport (Bilsland, Sahai et al. 2010).

The second project addressed mitochondrial transport in naturally occurring axon pruning during development. As axonal transport is considered to be involved in global axonal dystrophy in a variety of neurodegenerative disorders, it could potentially also be involved in the local elimination of individual axon branches. Axonal transport could mediate local distribution of resources and thus have a regulatory function in the competition between converging inputs.

In this thesis transport measurements were based on transgenic mice that express mitochondrially targeted cyan fluorescent proteins under a neuronal promoter (*thy1-MitoCFP* mice) (Misgeld, Kerschensteiner et al. 2007). Mitochondrial transport was imaged in acute nerve-muscle explants (Kerschensteiner, Reuter et al. 2008). Using this approach, it was possible to analyze temporal and spatial aspects of transport in the complex environment of degenerating and developing axons.

Material and Methods

Transgenic mouse lines

Imaging mitochondrial transport in motor axons is based on the use of several transgenic mouse lines.

Thy1-MitoCFP mice express mitochondrially targeted fluorescent proteins under the neuronal *thy1*-promoter (Misgeld, Kerschensteiner et al. 2007). Visualizing mitochondria specifically in neurons allows investigation of these organelles in vivo and in living tissue on a single-axon level. Heterozygous *thy1-MitoCFP^{C}* mice were utilized for experiments from postnatal day 20 (P20). In this mouse line mitochondria contain relatively low levels of cyan fluorescent proteins (CFP). Experiments from P7 to P20 were performed with the *thy1-MitoCFP^{K}* line. This mouse line expresses higher levels of CFP and is therefore most suitable for imaging in young animals, when mitochondria in *thy1-MitoCFP^{C}* are not yet bright enough. Homozygous *thy1-MitoCFP^{K}* mice develop a light tremor at the age of several months. Therefore use of this line is limited to heterozygous and young animals, which appear to be healthy. *Thy1-MitoCFP* lines (*thy1-MitoCFP^{C}*) can be ordered from The Jackson Laboratory, Bar Harbor, ME. Others (*thy1-MitoCFP^{K}*) are available through our lab.

The morphology of motor axons in their normal milieu can be imaged in transgenic mice expressing cytoplasmic yellow fluorescent proteins (YFP) under the *thy1*-promoter (*thy1-YFP*) (Feng, Mellor et al. 2000). *Thy1-YFP^{16}* is a line with almost 100% of α-motor neurons stained, in *thy1-YFP^{H}* mice only a subset of α-motor neurons express fluorescent proteins.

Transgenic mice expressing mutant forms of the enzyme Cu/Zn superoxide dismutase (SOD1) are used as models for the neurodegenerative disease amyotrophic lateral sclerosis (ALS). Mutations in the SOD1 gene are responsible for approximately 20% of all familial ALS cases in humans. Motor neuron pathology and clinical symptoms in SOD1-mutant mice are similar to those seen in patients with ALS. Different point-mutations result in the expression of either active or inactive forms of the enzyme and influence the phenotype of the disease. Various mouse lines also differ in their genomic *SOD1* copy numbers. We obtained our SOD1-mutant mice from The Jackson Laboratory. Table 1 shows characteristics of our most important SOD1 mouse lines (Marinkovic, Reuter et al. 2012).

	Enzyme function	Disease onset [months]		ΔCT value in quantitative PCR
		Weight loss	Reduced performance in grid test	
SOD^{G93A}	Active	3	3	7.1
SOD^{G85R}	Inactive	9	9.5	5.8
SOD^{WT}	Wild-type, active	None	None	6.2

Table 1: Characteristics of the most important SOD1 mouse lines used in our laboratory; phenotyping and quantitative PCR were performed by P. Marinkovic and M. Brill

Experiments in this thesis were performed on one of the most commonly used mouse lines, *SOD^{G93A}*. Those mice express high copy numbers of SOD1 with an amino acid substitution from glycine to alanine at position 93. Heterozygous *SOD^{G93A}* mice show progressive weight loss, weakness, tremor, dragging of the hind limbs and loss of coordination around P90 (Gurney, Pu et al. 1994). By 120–150 days of age, mice demonstrate rear limb paralysis and were sacrificed for ethical reasons. Onset of symptoms and lifespan are dependent on the type of mutation, genomic copy number and genetic background (Alexander, Erwin et al. 2004, Heiman-Patterson, Deitch et al. 2005).

For details on mouse breeding, refer to Appendix - Protocols.

All animal work conformed to institutional guidelines and was approved by the Animal Study Committee of the Regierung von Oberbayern.

Acute nerve-muscle explants of the triangularis sterni muscle (Kerschensteiner, Reuter et al. 2008)

Imaging motor axons and mitochondrial transport was performed in acute nerve-muscle explants of a thin muscle located at the inside of the thorax, the triangularis sterni muscle (TS). These explants could be maintained alive for several hours and allowed high-resolution imaging of peripheral motor axons. Movement artefacts were minimized compared to *in vivo* experiments since there was no pulse or respiration. The triangularis sterni muscle is very thin and consists of only a few layers of muscle fibers. As a consequence the innervating motor axons run superficially and allow imaging of small structures like mitochondria. The explant could be dissected without damaging the muscle because it originates and inserts on bony components of the rib cage. During the preparation of the TS explants, motor axons of intercostal nerves were separated from their cell bodies in the spinal cord. This limited the lifespan of explants (Wallerian degeneration of transected axons sets in after 12-24h (Coleman

and Freeman 2010)) and the time axonal transport could be imaged (delivery of cargoes from the disconnected soma was stopped) (Kerschensteiner, Reuter et al. 2008).

Explantation of the triangularis sterni muscle (Kerschensteiner, Reuter et al. 2008)

The mice were lethally anaesthetized (ketamine-xylazine intraperitoneally (i.p.) for pubs, Isoflurane for adult mice) and the fur was sprayed with 70% ethanol to avoid contaminating the dish with hair. Dissection of the TS was different for young and adult mice: in animals younger than P20 both sides of the thorax were explanted, in adult mice only a hemithorax was placed in the dish.

Preparation of young mice (<P20):

The animals were decapitated with large medical scissors. The abdomen was transected below the ribs to isolate the thorax. Skin, back muscles, scapulae and pectoral muscles were removed to obtain the thorax. The thorax was transferred to a dish with cooled carbogen-bubbled Ringer's solution; further dissection was performed under a stereo microscope. By means of small-angled spring scissors, the ribs were transected close to the costovertebral joints, to preserve the longest possible length of motor axons. The diaphragm was severed around the entire circumference of the thorax. Vertebral column, diaphragm and thoracic viscera were removed from the rib-cage. Remnants of pleura, diaphragm (inside) and pectoral muscles (outside) were removed to obtain the isolated thorax preparation. The thorax was placed in a Sylgard-coated 3.5-cm dish with its inner side up, and secured with fine minuten pins (the preparation was slightly stretched and flat). The whole muscle was covered with carbogen-bubbled medium at all times.

Preparation of the left hemithorax of adult mice (>P20):

The animals were killed by cervical dislocation. By means of large medical scissors a midline incision of the skin over the sternum and two incisions parallel to the lower borders of the rib cage were performed. Skin and pectoral muscles of the left side of the thorax were removed. In the back, the muscular attachments of the scapula to the thorax were cut, to expose the left side from the sternum to the vertebral column. The abdominal wall was opened following the left lower thorax border all the way to the vertebral column. The diaphragm was opened beneath the xiphoid cartilage using small-angled spring scissors and was dissected off its costal insertions along the left circumference of the thorax. On the right-hand side of the sternum the ribs were cut from the xiphoid cartilage to the manubrium sterni. The left ribs were cut off

the vertebral column near their insertion. By cutting through the remaining bridge of tissue above the sternum, the left half of the thorax was mobilized. The explanted hemithorax was transferred to a dish with cooled carbogen-bubbled Ringer's solution. Further dissection was performed under a stereo microscope. Remnants of thymus, pleura, diaphragm (inside) and pectoral muscles (outside) were removed. The thorax was pinned into a Sylgard-coated 3.5-cm dish with fine minuten pins, to gently stretch the muscle.

Maintenance of the explant and image acquisition (Kerschensteiner, Reuter et al. 2008)

Sufficient supply of oxygen and energy substrates was ensured during the experiment to keep the explant in viable condition. During time-lapse imaging the explant was superfused with prewarmed carbogen-bubbled Ringer's solution (flow rate 1ml/min). The temperature was stabilized at 32–37°C. This was achieved by surrounding the dish with a heating ring and superfusing it with prewarmed Ringer's solution. For the latter, an in-line heater, which was feedback-controlled by a temperature probe, was integrated into the superfusion system.

Time-lapse imaging of motor axons or synapses was performed at an Olympus BX51WI upright fluorescence microscope with objective focusing and a custom-built x–y stage. The microscope was equipped with an automated filter wheel (Sutter) and filters for fluorescent proteins (ET F46-001 for CFP, ET F46-003 for YFP, ET F46-008 for TxRED; AHF Analysentechnik, Germany). To reduce photo-damage, the amount of light was kept at the lowest possible level. Therefore, a fast software-controlled shutter was used and neutral density and infrared-blocking filters were inserted in the light path (U25ND25 and U25ND6; Olympus). The system was controlled by TillVision software.

An overview of the innervation pattern was gained with a 4x/ N.A. 0.13 air objective and a 20x/ N.A. 0.5 water-immersion dipping cone objective and fluorescence excitation. Mitochondria in motor axons or synapses of interest were imaged with a 100x/ N.A. 1.0 water-immersion dipping cone objective. Time-lapse imaging was performed by taking series of images with an acquisition rate of 1/sec (exposure time 500ms) with the lowest acceptable illumination intensity, to avoid bleaching and resulting phototoxicity. The pixel size in the image plane was adjusted by binning 4 pixels to achieve a near-Nyquist spatial sampling rate of 0.128µm/pixel.

Mitochondrial transport in intercostal nerves:

Mitochondrial transport in *SOD*^{G93A} mice and controls was imaged in intercostal nerves in a region where the axons ran superficially and were only covered by parietal pleura. Most motor axons have not sent off branches proximal to the imaged region. Series of approximately 300 images (300 seconds) were recorded from different intercostal nerves. Time, temperature and intercostal space was documented for each recording. Axonal morphology in the imaged region was documented in *thy1-YFP* animals.

Mitochondrial transport in terminal axon branches:

Mitochondrial transport in developing motor axons was imaged in terminal branches (distal of the last branch-point) in the endplate band of the triangularis sterni muscle. Mitochondrial transport was recorded in superficial axon branches for a total of 50-60 minutes. After completion of the time-lapse recording, axonal morphology and innervation pattern was documented by acquiring image stacks with lower magnification (20x, 4x) to re-identify the region after tissue fixation. Mitochondrial transport measurements were limited to 90 minutes after sacrificing the animal, to avoid a drop in cargo delivery.

Images were acquired using a cooled CCD camera (SensicamQE (Cooke), recorded onto electronic media (TillVision software) and analyzed offline (ImageJ/Fiji, Photoshop (Adobe)).

Fixation, dissection and staining of the muscle (Kerschensteiner, Reuter et al. 2008)

The tissue was fixed in 4% paraformaldehyde (PFA) in 0.01M phosphate-buffered saline (1x PBS) for 1.5h at 4°C. Fixed explants could be stored in 1x PBS/0.1% sodium azide (NaN_3) at 4°C. After fixation the triangularis sterni muscle was dissected off the rib cage for subsequent stainings and confocal imaging:

Under a dissection microscope the sternum was cut away with a razor blade (the cut was placed between the internal mammary vessels and the sternum). The ribs were trimmed near the cartilage-bone transition to obtain a piece of tissue corresponding to the triangularis sterni muscle. By means of a fine hypodermic needle on a syringe as dissection tool the thin muscle was detatched from the ribs and intercostal muscles. The muscle was then cleaned from fat and connective tissue without ripping off the nerves.

Stainings of postsynaptic acetylcholine receptors were performed by applying Alexa594-conjugated α-bungarotoxin (BTX) (according to protocols in the Appendix).

Stained muscles were washed in 1x PBS, mounted on a slide with antifading medium (Vectashield, Vector Laboratories) and cover-slipped. Slides were flattened between a metal plate and small magnets overnight. Finished slides were kept at -20°C.

Time-lapse analysis (Kerschensteiner, Reuter et al. 2008)

The primary set of data consisted of recorded series of images. This file was processed and x-y aligned using ImageJ (http://rsbweb.nih.gov/ij/) with the 'stackreg' plugin (http://bigwww.epfl.ch/thevenaz/stackreg/). The resulting image series was cropped and stored as a stacked tiff format.

Amount of transport (mitochondrial flux) was analyzed manually by counting how many mitochondria passed an axonal cross-section per minute in anterograde and retrograde direction. All moving, fluorescently labeled objects were included in the counting (irrespective of whether they were in focus or not). Analysis of SOD^{G93A} mice *vs.* controls was performed blinded in P10 and P20 mice. In animals older than P20 the genotype was revealed by different mitochondrial morphology.

Velocity of moving mitochondria was analyzed in the same set of data. Average mitochondrial velocity was determined by measuring the distance a mitochondrion had covered in a certain time. A frequency distribution was obtained by measuring the distance a mitochondrion had covered within one second (frame-by-frame analysis).

Mitochondrial morphology was objectified with the so-called 'shape factor', which is defined as the ratio of mitochondrial length to width. Shape factor analysis was performed by Petar Marinkovic (Institut für Neurowissenschaften, TU München) in the set of data obtained for time-lapse analysis of mitochondrial transport in this study.

Confocal imaging (Kerschensteiner, Reuter et al. 2008)

High-resolution image stacks of fixed triangularis sterni muscles were acquired on an upright confocal microscope (FV1000, Olympus) equipped with 60x/ N.A. 1.42 and 20x/ N.A. 0.85 oil objectives, and 10x/ N.A. 0.40 and 4x/ N.A. 0.13 air objectives.

For illustration, spectral channels of confocal image stacks were combined and pseudo-coloured in Photoshop-software. Gamma was adjusted non-linearily to enhance low-intensity objects.

To determine the percentage of denervated neuromuscular junctions in triangularis sterni muscles of *SOD^{G93A}, thy1-YFP^{16}* mice, postsynaptic acetylcholine receptors were stained with Alexa594-conjugated α-bungarotoxin. Neuromuscular junctions were imaged by confocal microscopy (20x/ N.A. 0.85 oil objective) and subdivided into three categories: 'completely innervated' (postsynaptic structures (BTX) were completely covered by presynaptic nerve terminals (YFP)), 'partially innervated' (postsynaptic receptors were in part covered by axon-endings) and 'denervated' (BTX-labeled regions without presynaptic structures), refer to figure 2.

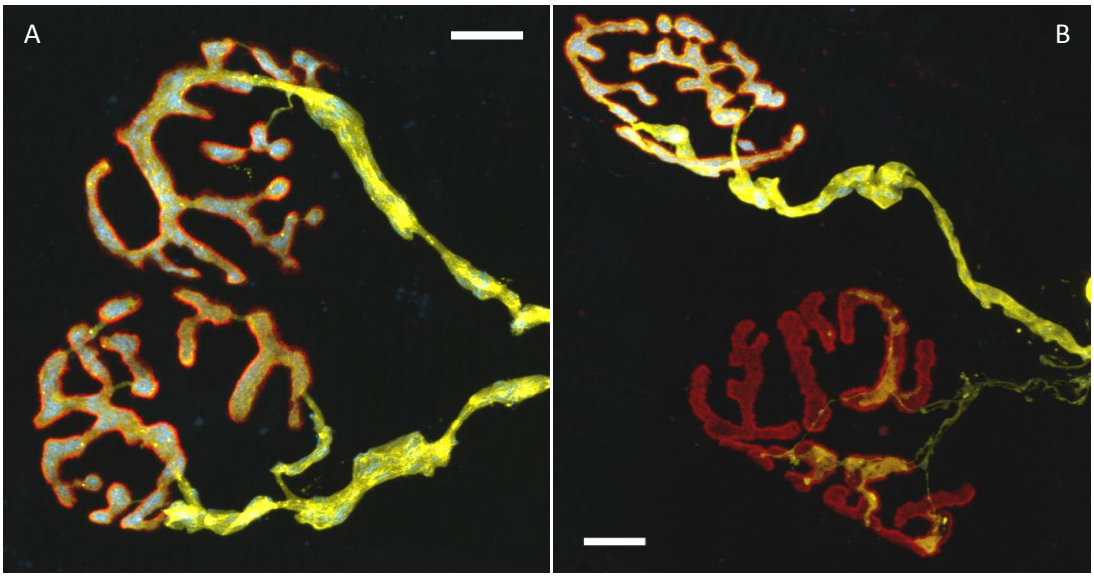

Figure 2: (A) Two completely innervated neuromuscular junctions in a *thy1-YFP^{16}*, *thy1-MitoCFP^{C}* control, (B) one partially innervated (bottom) and one completely innervated neuromuscular junction (top) in a P120 *SOD^{G93A}*, *thy1-YFP^{16}*, *thy1-MitoCFP^{C}* mouse (axons in yellow, postsynaptic receptors in red, mitochondria in cyan; triangularis sterni muscle; scale bars 10µm)

After imaging mitochondrial transport in terminal axon branches during development, the tissue was fixed and stained with Alexa594-BTX. A majority of NMJs and axon branches of interest were re-identified and imaged with high resolution by confocal microscopy (60x/ N.A. 1.42 oil objective).

Axon branches in the process of synapse elimination were categorized according to their stage in the elimination process: *(1)* axon branches that had won all their competitions and innervated a singly innervated muscle fiber (*'winner' branches*), *(2)* axon branches that had lost contact to the synapse and ended in a retraction bulb (*'loser' branches*), *(3)/(4)* axon branches going to doubly innervated muscle fiber and showing morphologic characteristics of *putative 'winners' or 'losers'* ('asymmetric' branches), *(5)* axon branches going to a muscle fiber that

was innervated by two morphologically unremarkable branches (*'symmetric' branches*) (refer to figure 3).

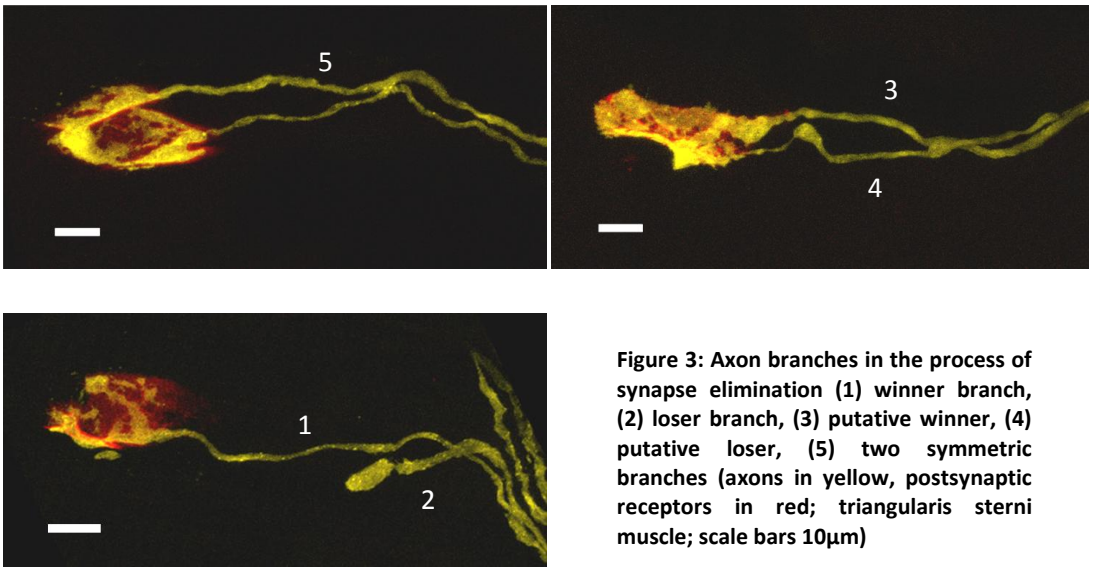

Figure 3: Axon branches in the process of synapse elimination (1) winner branch, (2) loser branch, (3) putative winner, (4) putative loser, (5) two symmetric branches (axons in yellow, postsynaptic receptors in red; triangularis sterni muscle; scale bars 10µm)

Statistical analysis

Amount of transport in intercostal nerves was considered to be normally distributed. Unless indicated elsewise, values are average values +/- standard errors of the mean (SEM). P-values were calculated by performing *t*-tests. Differences were considered to be significant if $p<0.05$. Statistical analyses were performed with SPSS (version 10), tables and graphs were compiled with Microsoft Excel 2007.

Results

Mitochondrial transport in acute explants of intercostal nerves

In order to establish a reproducible method to quantify mitochondrial transport in axons, time-lapse analyses were performed in transgenic mice (*thy1-MitoCFP*^{C} and *thy1-MitoCFP*^{K}) of different ages. We chose to measure transport in intercostal nerves of acute thoracic explants. Those measurements served as controls for subsequent experiments.

Axonal mitochondria were either immobile or moved in anterograde or retrograde direction. 8.9 mitochondria (mito) passed an axonal cross-section per minute (min) (average number of anterograde and retrograde moving mitochondria per minute in 314 axons from n=30 mice between postnatal day (P) 10 and P122, SEM are displayed in table 2).

6.0 mito/min moved in anterograde direction (68%), 2.9 moved in retrograde direction (32%; n=30 mice). The ratio of anterograde to retrograde transport was 2.1 to 1.The average number of transported mitochondria was constant in mice at different ages. Figure 4 shows a time course of anterograde and retrograde transport in mice between P10 and P122 (n=30 mice). Average velocity of moving mitochondria was 0.88µm/sec in anterograde direction and 0.90µm/sec in retrograde direction.

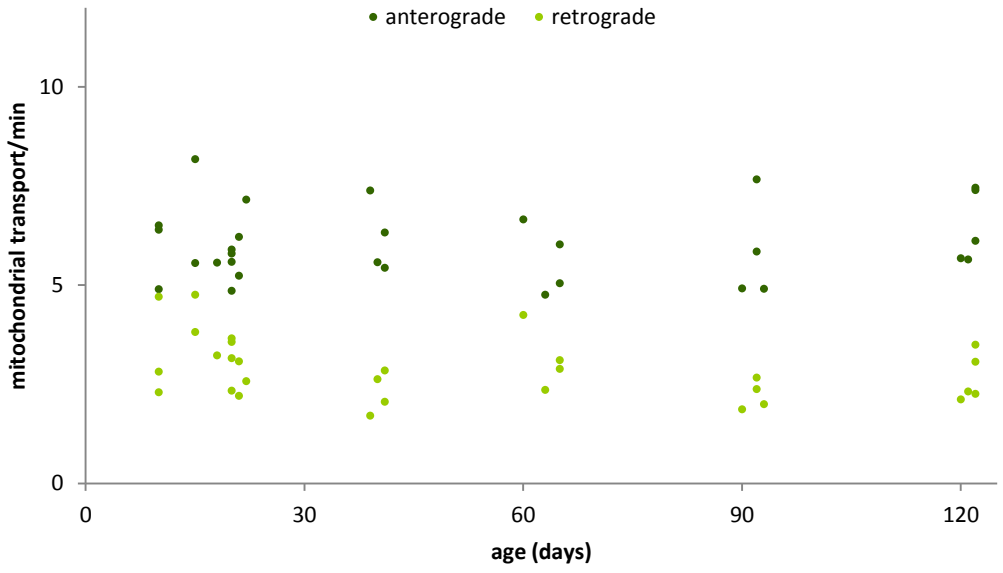

Figure 4: Time course of average anterograde and retrograde mitochondrial transport rates (mitochondria per minute per axon) in intercostal nerves from *thy1-MitoCFP* mice between P10 and P122 (n=30 mice)

Part 1: Mitochondrial transport in motor axons of a *SOD^{G93A}* mouse model

Amyotrophic lateral sclerosis is characterized by progressive die-back neuropathy of whole motor units and sprouting with reinnervation by others (Frey, Schneider et al. 2000). Several studies suggest a role of mitochondrial pathology and axonal transport deficits in human ALS and SOD1-based models of the disease (Breuer, Lynn et al. 1987, Sasaki and Iwata 1996, Warita, Itoyama et al. 1999, Williamson and Cleveland 1999, Pun, Santos et al. 2006, De Vos, Chapman et al. 2007, Bilsland, Sahai et al. 2010, Vande Velde, McDonald et al. 2011, Magrane, Sahawneh et al. 2012). However, it remains unclear whether transport deficits contribute to ALS pathogenesis and how they correlate with disease initiation or progression.

In the literature distinct muscles have been described to show a different vulnerability to motor axon degeneration in *SOD^{G93A}* mice (Frey, Schneider et al. 2000). In my work I concentrated on the triangularis sterni muscle, which is innervated by motor axons from intercostal nerves. Advantages of this muscle are discussed in the section 'Discussion - Methodological considerations'. To investigate the time course of axonal degeneration, the percentage of denervated neuromuscular junctions was determined in triangularis sterni muscles (TS) from *SOD^{G93A}, thy1-YFP^{16}* mice at P60, P90 and P120. Neuromuscular junctions were imaged by confocal microscopy and classified as 'completely innervated', 'partially innervated' or 'denervated' (refer to section 'Materials and Methods – Confocal imaging'). At P60 99.6% of the NMJs in the TS were completely innervated and 0.4% were partially innervated (1461 NMJ from n=3 mice). At P90 98.7% of the NMJ were completely innervated, 1.2% were partially innervated and 0.1% were denervated (1658 NMJ from n=5 mice). In late stages of the disease at P120 69.3% of the NMJ were completely innervated, 14.2% were partially innervated and 16.5% were denervated (2031 NMJ from n=4 mice) (figure 5).

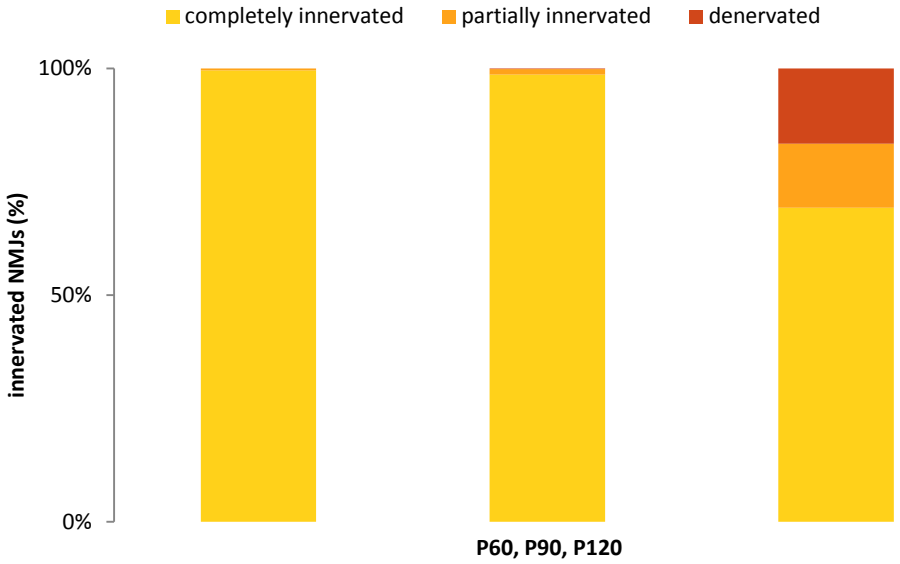

Figure 5: Time course of neuromuscular denervation in triangularis sterni muscles of *SOD^{G93A}*, *thy1-YFP^{16}* mice (analysis of 1461/1658/2031 NMJs from n=3/5/4 mice for P60/P90/P120)

To examine the incidence of transport deficits in an animal model of ALS, mitochondrial transport was quantified in acute explants of intercostal nerves from *SOD^{G93A}*, *thy1-MitoCFP* double-transgenic mice. Transport measurements in wild-type *thy1-MitoCFP* mice served as controls. Values indicate average transport (mitochondria/min), n=number of mice, SEM are displayed in table 2.

At age P90 first symptoms developed in our *SOD^{G93A}* mouse line, usually affecting the hindlimbs first (Gurney, Pu et al. 1994). In the triangularis sterni muscle no pronounced denervation was apparent at this stage of the disease (figure 5). In contrast, total mitochondrial transport (anterograde plus retrograde) in intercostal nerves of P90 *SOD^{G93A}* mice was significantly reduced (4.1 mito/min in *SOD^{G93A}*, 87 axons from n=6 mice, *vs.* 8.1 mito/min in controls, 39 axons from n=4 mice; p=0.002, *t*-test). Anterograde and retrograde transport were both significantly reduced (p=0.002 for anterograde transport and p=0.004 for retrograde transport). Analyses of transport on the level of individual axons showed heterogeneities within *SOD^{G93A}* axons and controls (figure 6).

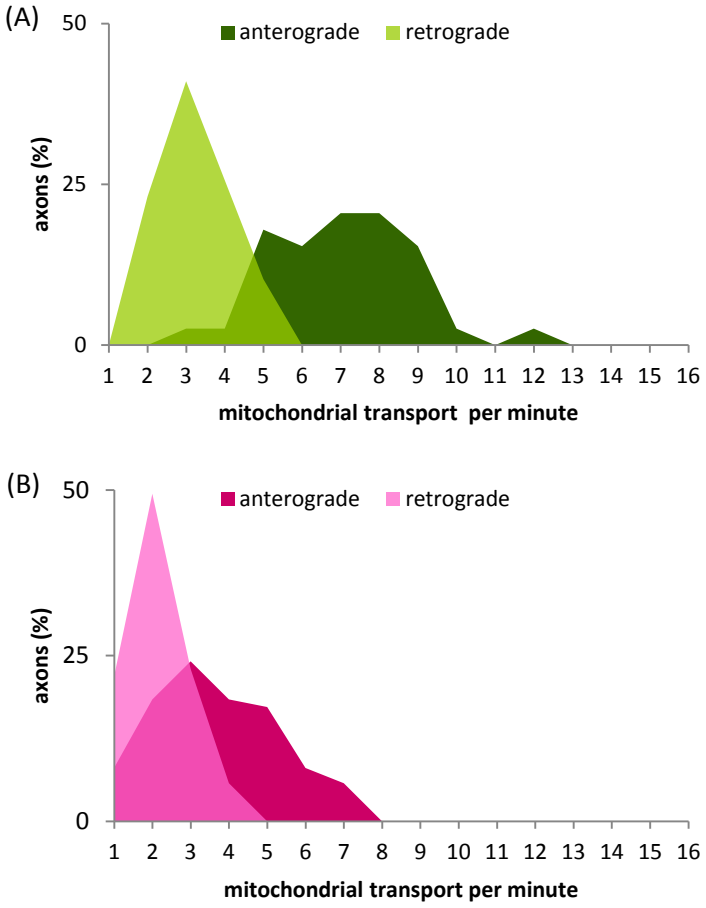

Figure 6: Frequency distribution of anterograde and retrograde mitochondrial flux in intercostal nerves of P90 wild-type controls (A) and *SOD^{G93A}* mice (B), (39/87 axons from n=4/6 wild-type/*SOD^{G93A}* mice)

To explore the onset of abnormal mitochondrial morphology and transport deficits, time-lapse imaging was performed in *SOD^{G93A}, thy1-MitoCFP* mice of different ages. The temporal course of transport is displayed in table 2 and figure 7. At the age of P120, *SOD^{G93A}* animals were sacrificed for ethical reasons. It appears that anterograde and retrograde mitochondrial transport were not significantly different in *SOD^{G93A} vs.* wild-type mice at P10 (total transport of 9.3 mito/min in *SOD^{G93A}*, 41 axons from n=6 mice, *vs.* 9.21 mito/min in controls, 28 axons from n=3 mice; p=0.95 for total transport, p=0.76 for anterograde transport, p=0.69 for retrograde transport). At P20, more than 2 months before the onset of symptoms, transport was reduced in *SOD^{G93A}* mice (total transport of 7.2 mito/min in *SOD^{G93A}*, 83 axons from n=6 mice, *vs.* 8.7 mito/min in wild-type mice, 96 axons from n=8 mice; p=0.008). Anterograde transport was significantly diminished at P20 (p=0.002), whereas the difference in retrograde transport was not significant (p=0.362), refer to figure 7. At P40 total transport in *SOD^{G93A}* was 6.0 mito/min (122 axons from n=9 mice) *vs.* 8.5 mito/min (41 axons from n=4 mice) in controls (p=0.019). Anterograde transport was significantly reduced (p=0.008), whereas the difference

in retrograde transport was again not significant (p=0.311). At P60 total transport, anterograde and retrograde transport were reduced significantly in *SOD*^{G93A} (p=0.003 for total transport, p=0.002 for anterograde transport, p=0.013 for retrograde transport). At P120, which is during the end-stage of the disease, total transport in *SOD*^{G93A} mice had declined to 4.0 mito/min, compared to 9.1 mito/min in controls (p=0.002). Anterograde and retrograde transport were both significantly reduced in *SOD*^{G93A} (p=0.001 for anterograde transport, p=0.036 for retrograde transport). In summary, my data imply that total mitochondrial transport in intercostal nerves from *SOD*^{G93A} mice was considerably reduced months before symptoms emerge or denervation was apparent. Separate analyses of anterograde and retrograde transport revealed that anterograde transport of mitochondria was significantly reduced at P20, whereas statistically significant differences in retrograde transport could first be detected at P60.

wild-type	transport (mito/min)		
age	anterograde (+/- SEM)	retrograde (+/- SEM)	total (+/- SEM)
P10	5.9 (+/- 0.5)	3.3 (+/- 0.7)	9.2 (+/- 1.0)
P20	5.8 (+/- 0.2)	3.0 (+/- 0.2)	8.7 (+/- 0.3)
P40	6.2 (+/- 0.5)	2.3 (+/- 0.3)	8.5 (+/- 0.4)
P60	5.6 (+/- 0.4)	3.2 (+/- 0.4)	8.8 (+/- 0.8)
P90	5.8 (+/- 0.8)	2.2 (+/- 0.2)	8.1 (+/- 1.0)
P120	6.5 (+/- 0.4)	2.7 (+/- 0.3)	9.1 (+/- 0.6)

SOD^{G93A}	transport (mito/min)		
age	anterograde (+/- SEM)	retrograde (+/- SEM)	total (+/- SEM)
P10	5.7 (+/- 0.4)	3.6 (+/- 0.3)	9.3 (+/- 0.6)
P20	4.4 (+/- 0.3)	2.7 (+/- 0.2)	7.2 (+/- 0.4)
P40	4.0 (+/- 0.4)	2.0 (+/- 0.2)	6.0 (+/- 0.6)
P60	2.9 (+/- 0.4)	1.6 (+/- 0.3)	4.5 (+/- 0.6)
P90	2.8 (+/- 0.4)	1.2 (+/- 0.2)	4.1 (+/- 0.6)
P120	2.5 (+/- 0.6)	1.5 (+/- 0.4)	4.0 (+/- 1.0)

p-value (*t*-test)	transport *wild-type vs.* *SOD*^{G93A}		
age	anterograde	retrograde	Total
P10	0.755	0.686	0.952
P20	**0.002**	0.362	**0.008**
P40	**0.008**	0.311	**0.019**
P60	**0.002**	**0.013**	**0.003**
P90	**0.002**	**0.004**	**0.002**
P120	**0.001**	**0.036**	**0.002**

Table 2: Time course of anterograde, retrograde and total mitochondrial transport in intercostal nerves of wild-type controls and *SOD*^{G93A} mice between P10 and P120 (average values +/- SEM); corresponding p-values (significant p-values bold)

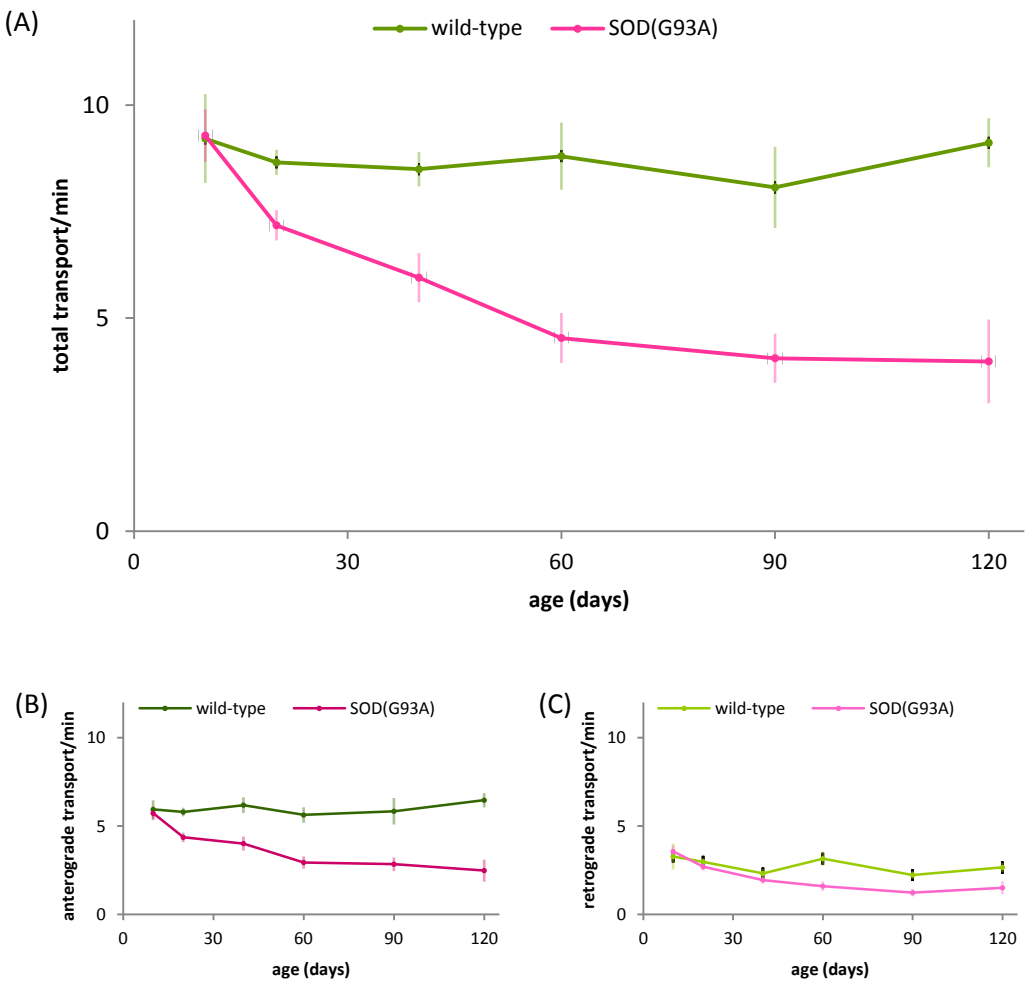

Figure 7: Time course of total (A), anterograde (B) and retrograde (C) mitochondrial transport in intercostal nerves of wild-type controls and *SOD*^{G93A} mice between P10 and P120 (average values +/- SEM)

To further investigate another parameter of axonal transport, mean velocity of moving mitochondria in P90 *SOD*^{G93A} mice was measured and compared to controls. Mitochondria in *SOD*^{G93A} animals moved on average slower than in wild-type mice (anterograde direction: 0.63µm/sec for *SOD*^{G93A} *vs.* 0.88µm/sec for controls, 165/127 mitochondria from n=3/3 mice; retrograde direction: 0.68µm/sec for *SOD*^{G93A} *vs.* 0.90µm/sec for controls, 123/105 mitochondria from n=3/3 mice, figure 8). Frame-by-frame analysis of anterograde transport revealed a frequency distribution of mitochondrial velocity. In P90 *SOD*^{G93A} mice there was higher frequency of pauses, an increase in the frequency of intermediate velocities, and a reduction in maximum velocity (1064/984 seconds of 48/50 mitochondria analyzed for *SOD*^{G93A}/controls, figure 9).

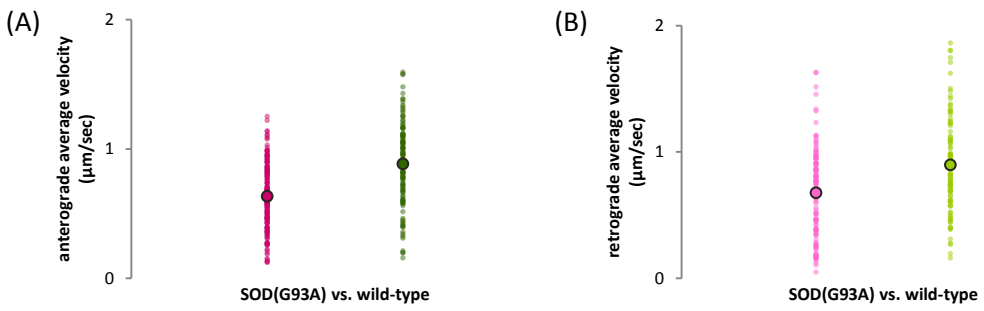

Figure 8: Average anterograde (A) and retrograde (B) mitochondrial velocity in intercostal nerves of *SOD*^{G93A} mice and wild-type controls at P90 (one transparent data point refers to average velocity of one mitochondrion, analysis of 165/127 mitochondria from n=3/3 *SOD*^{G93A}/wild-type mice)

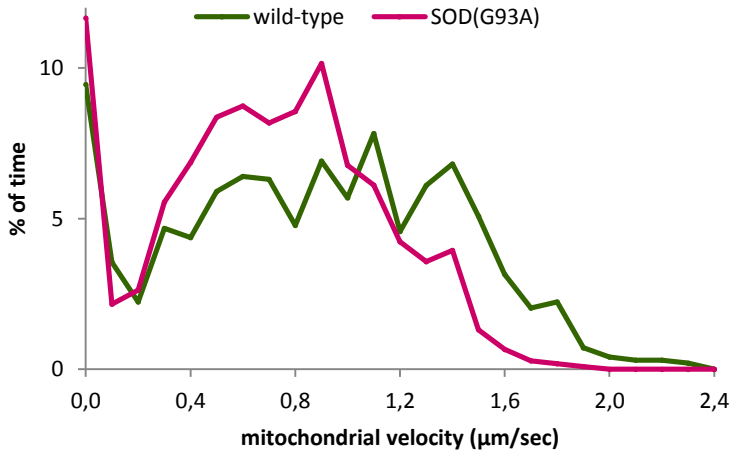

Figure 9: Frequency distribution of anterograde mitochondrial velocity in intercostal nerves of *SOD*^{G93A} mice and wild-type controls at P90 (1064/984 seconds of n=48/50 mitochondria analyzed for *SOD*^{G93A}/wild-type mice)

Mitochondria in motor axons of *SOD*^{G93A}, *thy1-MitoCFP*^{C} animals showed an altered morphology, they appeared shorter and rounder than in *thy1-MitoCFP*^{C} controls (figure 10). This discrepancy in mitochondrial morphology was quantified by calculating a 'shape factor'. Shape factor was defined as the ratio between mitochondrial length and width, resulting in higher values for long mitochondria and lower values for short and round mitochondria. Shape factor analysis was performed by Petar Marinkovic (Institut für Neurowissenschaften, Technische Universität München) in the set of data I obtained for time-lapse analysis of mitochondrial transport. At P90 the average shape factor in *SOD*^{G93A} animals was 6.1 compared to 9.9 in controls. The time course of shape factors (P10 – P120) is displayed in figure 10.

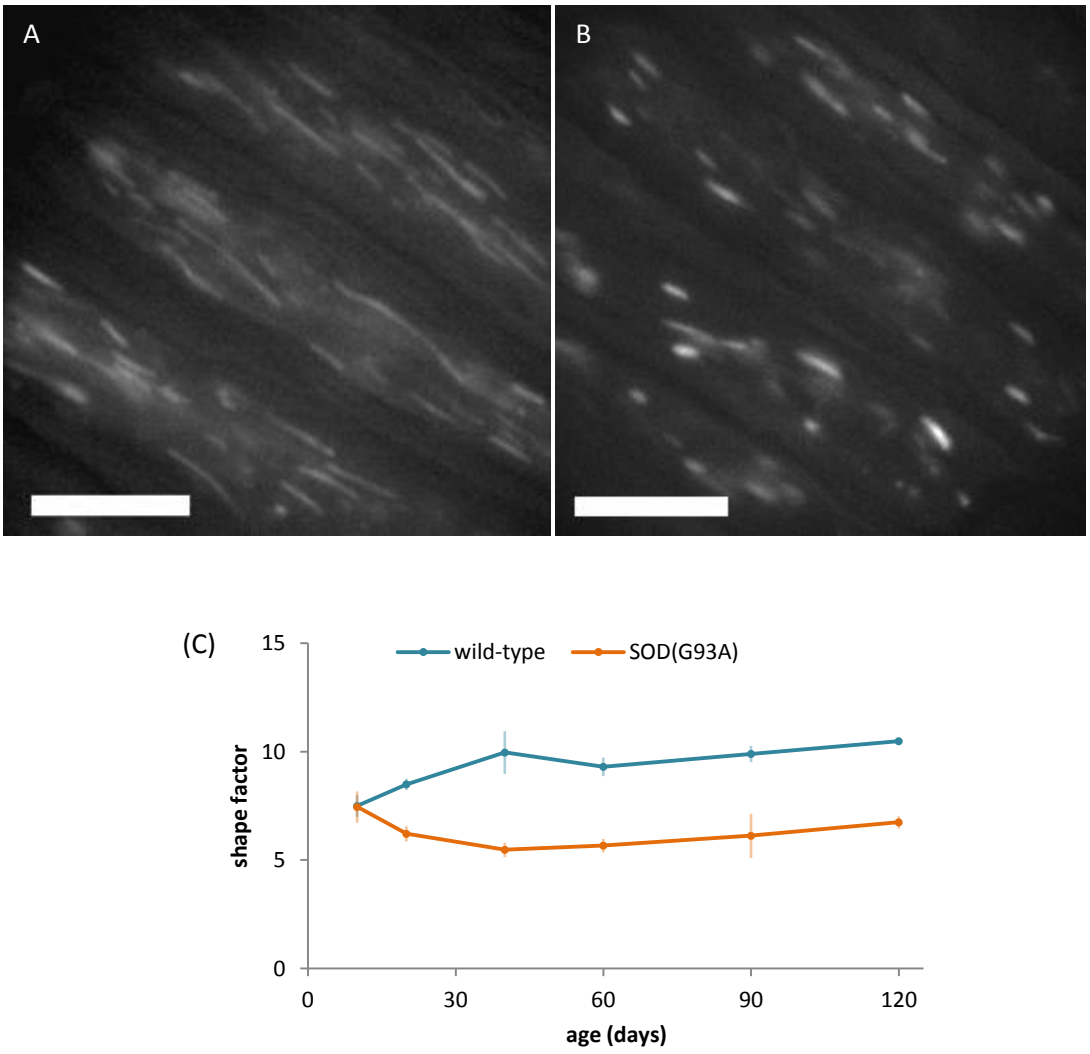

Figure 10: Mitochondria in intercostal axons in a *thy1-MitoCFP* control (P90) (A), a *SOD^{G93A}*, *thy1-MitoCFP* mouse (P90) (B) (epifluorescence microscopy; scale bars 10µm), (C) shape factor analysis of mitochondria in intercostal nerves of wild-type controls and *SOD^{G93A}* mice (average values +/- SEM; shape factor analysis was performed by P. Marinkovic)

Different muscles have been described to show a distinct vulnerability to motor axon degeneration in ALS and *SOD^{G93A}*. In human patients, for unknown reasons, functioning of extraocular muscles (EOM) is often not impaired even in late stages of the disease (Donaghy, Thurtell et al. 2011). Accordingly, extraocular muscles (M. obliquus superior, M. rectus superior) in P120 *SOD^{G93A}, thy1-MitoCFP, thy1-YFP* mice lacked denervated NMJs. Mitochondria in these axons looked morphologically unremarkable in confocal analysis (figure 11), suggesting an association of mitochondrial morphology with motor axon degeneration.

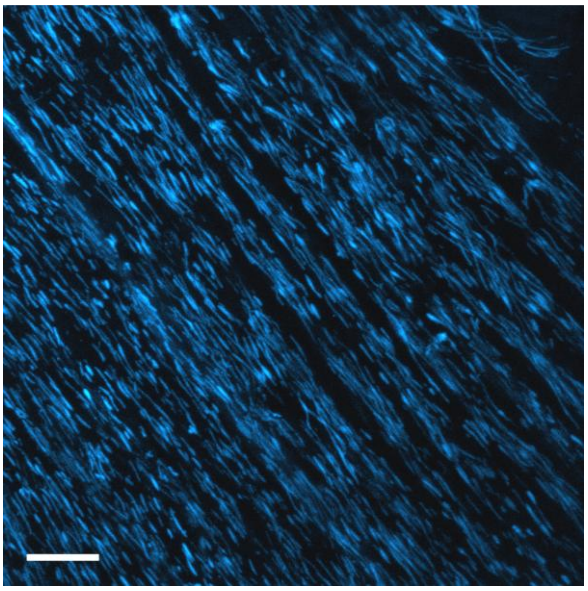

Figure 11: Mitochondria in axons innervating the superior rectus muscle (oculomotor nerve, cranial nerve III) in a *SOD^{G93A}*, *thy1-MitoCFP* mouse (P120) (confocal microscopy; scale bar 10µm)

Part 2: Mitochondrial transport in the development of the neuromuscular junction

In postnatal mammalian muscles several motor axon branches converge at the same NMJ. During the first weeks after birth many of these branches are eliminated, leaving each muscle fiber innervated by a single motor axon. Local distribution of resources within a motor neuron might be a decisive factor in the competition between axon branches. This resource could be neurotransmitters, trophic factors or organelles (e.g. mitochondria). Hence, a possible candidate for mediating axon elimination is disturbed axonal transport in retreating branches. To test this hypothesis, I measured mitochondrial transport in motor axon branches from *thy1-MitoCFP^{K}*, *thy1-YFP^{16}* pubs. Axon branches in the process of synapse elimination were categorized according to their stage in the elimination process (refer to section 'Material and Methods - Confocal imaging': 1. 'winner' branches, 2. 'loser' branches, 3./4. 'asymmetric' branches with putative winners and losers, 5. 'symmetric' branches in those the outcome could not be predicted).

Mitochondrial transport was measured in acute explants of triangularis sterni muscles from *thy1-YFP^{16}*, *thy1-MitoCFP^{K}* pubs (P7-P11). Terminal axon branches were imaged distally of the last branch-point close to the synapse or retraction bulb. Values indicate average transport (mitochondria/min) +/- SEM, n=number of axon branches. Axon branches going to a singly innervated muscle fiber ('winners') transported in average 0.09 (+/-0.01) mito/min in anterograde and 0.07 (+/-0.009) mito/min in retrograde direction (n=48), refer to figure 12 (A). Transport in axon branches undergoing elimination and ending in retraction bulbs ('losers') was deficient. However, it was not completely absent as 0.003 (+/-0.002) mito/min were

transported in anterograde and 0.004 (+/-0.002) mito/min were transported in retrograde direction (n=12), refer to figure 12 (B).

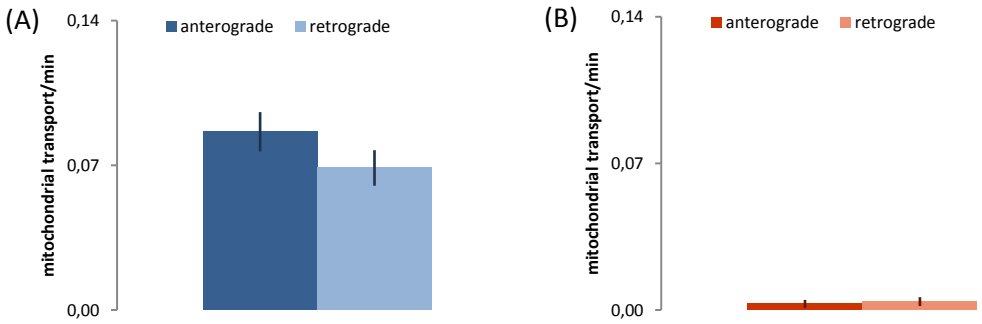

Figure 12: (A) Anterograde and retrograde mitochondrial transport in axon branches going to a singly innervated muscle fiber (n=48 axon branches), (B) Anterograde and retrograde mitochondrial transport in retreating axon branches ending in a retraction bulb (n=12 axon branches)

Before axon branches lose contact to the muscle fiber they show characteristic morphologic changes, like local thinning and swellings (consistent with local dystrophy). Most of these branches undergo elimination within the next hours or days (Keller-Peck, Walsh et al. 2001). To explore whether a mitochondrial transport deficit is apparent at this stage of synapse elimination, competitive 'asymmetric' branches were imaged. Branches going to an asymmetrically innervated muscle fiber and showing morphology of a future 'winner' transported 0.11 (+/-0.02) mito/min in anterograde and 0.08 (+/-0.01) mito/min in retrograde direction (n=29), refer to figure 13 (A). This transport was not significantly different from a definite 'winner' branch (p=0.244 for anterograde and p=0.477 for retrograde direction, *t*-test). In contrast, branches still connected to the synapse but showing morphology of a future 'loser' were already undersupplied with mitochondria (0.007 (+/-0.002) mito/min were transported in anterograde and 0.011 (+/-0.003) mito/min were transported in retrograde direction (n=29) (figure 13 (B). Thus, mitochondrial transport reduction could be observed before branches finally retreat from a synapse.

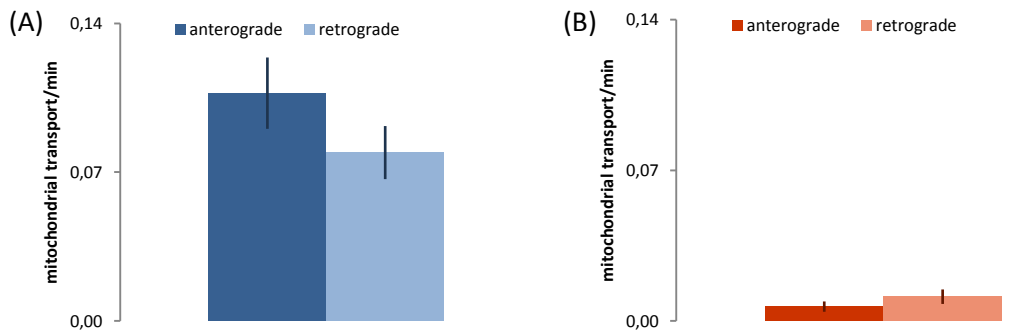

Figure 13: (A) Anterograde and retrograde mitochondrial transport in predicted 'winner' branches of asymmetrically innervated muscle fibers (n=29 axon branches), (B) Anterograde and retrograde mitochondrial transport in predicted 'loser' branches of asymmetrically innervated muscle fibers (n=29 axon branches)

In symmetrically innervated muscle fibers it was not possible to predict a 'winner' branch. Average transport in each axon branch was about half the rate compared to branches of singly innervated muscle fibers (0.04 (+/-0.006) mito/min were transported in anterograde and 0.03 (+/-0.004) mito/min were transported in retrograde direction (n=52), figure 14). This result at the same time shows that axonal transport of mitochondria is matched to the size of the supplied target on a branch-to-branch level.

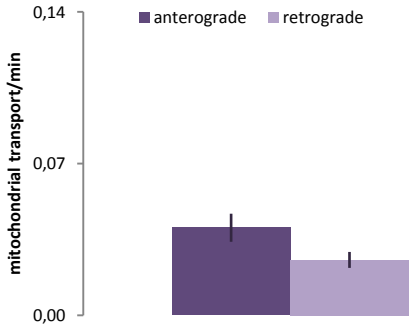

Figure 14: Anterograde and retrograde mitochondrial transport in axon branches of symmetrically double innervated muscle fibers (n=52 axon branches)

As axon branches undergoing elimination were in average thinner than persisting ones, we were interested in the degree of correlation between axon diameter and transport. Transport in branches of doubly innervated muscle fibers is displayed as a function of mean axon diameter (measured in confocal reconstructions of distal axon branches), refer to figure 15. We found statistical correlation between the two parameters (Pearson correlation coefficient of 0.59). This correlation was significant on a level of $p<0.01$. However, as can be seen from the graphics, it is not possible to predict one parameter by the other.

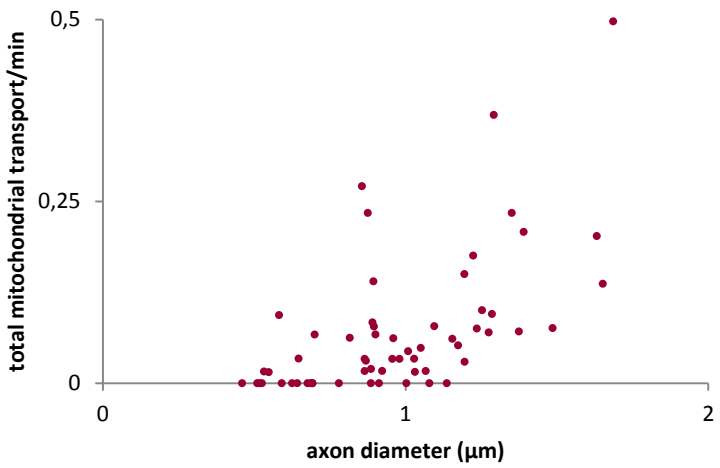

Figure 15: Correlation of total mitochondrial transport (anterograde + retrograde) with mean axon diameter (n=60 axon branches going to doubly innervated muscle fibers)

Discussion

Aim of this thesis was to investigate mitochondrial transport in a mouse model of motor neuron disease and in local elimination of individual axon arbors during development. The specific topics I wanted to investigate were:

Part 1: Mitochondrial transport in a mouse model of amyotrophic lateral sclerosis

Part 2: Mitochondrial transport in the postnatal development of the neuromuscular junction

Methodological considerations

One distinguishing feature of this work was the chosen methodological approach. Traditionally, axonal transport has been measured using assays of organelle density (Pun, Santos et al. 2006, Vande Velde, McDonald et al. 2011), transport of radioactively labeled proteins (Williamson and Cleveland 1999) and *in vitro* organelle tracking (De Vos, Chapman et al. 2007). In contrast, I measured mitochondrial flux in acutely explanted motor axons from *thy1-MitoCFP* animals. This method has several distinctive advantages over traditional approaches that were previously employed to measure axonal transport:

First of all, axonal transport could be directly visualized with high temporal resolution. Accordingly, a variety of transport parameters could be characterized (e.g. flux, velocity, frequency of pausing, etc.). Furthermore, our measurements were performed in living motor neurons within their natural habitat. This allowed mitochondrial flux to be interpreted in temporal and spatial context, e.g. in the course of a neurodegenerative disorder or during development. There is evidence that axonal transport *in vitro* differs from transport in *vivo* or in explants (e.g. the ratio of anterograde to retrograde transport, mitochondrial velocity (De Vos, Chapman et al. 2007, Misgeld, Kerschensteiner et al. 2007), emphasizing the necessity to confirm or confute *in vitro* data. Such differences in transport properties may result from altered myelination of neurons in cell culture (Bilsland, Sahai et al. 2010), as myelination can influence axoplasmic Ca^{++} levels and microtubule stability and therefore axonal transport parameters (Kirkpatrick and Brady 1994, Kiryu-Seo, Ohno et al. 2010).

Special features of our *ex vivo* experiments:

(1) Reproducibility: Transport rates in healthy animals were consistent with *ex vivo* data published by Misgeld et al. (2007). This consistency argues for a high reliability and objectivity of transport measurements in *thy1-MitoCFP* mice (Misgeld, Kerschensteiner et al. 2007). The reproducibility makes *thy1-MitoCFP* mice a useful approach to compare mitochondrial transport rates between different conditions (e.g. in a disease model).

(2) Quantifiability: Our results resulted in truly quantitative flux rates of mitochondria (rather than the more commonly obtained ratio of moving over resting mitochondria, which is e.g. influenced by mitochondrial density) and offered the possibility for objective comparisons and statistical analysis at the single axon level (e.g. in terms of statistical significance or correlations).

(3) Transport-to-morphology correlation: As transport of mitochondria was observed directly in individual axon branches, it could be correlated to morphological parameters (e.g. mitochondrial or axonal morphology, neuromuscular denervation).

(4) Cell-type specificity: As in *thy1-MitoCFP* animals mitochondria are labeled almost exclusively in neurons, transport measurements were not impacted by organelles in other cell types (e.g. glia or muscle fibers).

Advantages and disadvantages compared to *in vivo* measurements:

Our data were generated in acute explants of intercostal nerves and corresponding skeletal muscles (notably the triangularis sterni muscle). This *ex vivo* set-up exhibits advantages and disadvantages compared to *in vivo* measurements (e.g. in axons from the sternomastoid muscle or the tibialis nerve) (Kerschensteiner, Reuter et al. 2008).

The triangularis sterni muscle is a thin muscle (<5 layers of muscle fibers) located on the inside of the thorax. The innervating motor axons run superficially and allow precise and high-quality imaging of small structures like mitochondria. Due to its anatomical location, imaging in this muscle can only be performed in acute thoracic explants. Such explants exhibit the advantage that movement artefacts are generally minimized since there is no pulse or respiration. On the other hand, during preparation of the explants, intercostal nerves are separated from their cell bodies in the spinal cord. Because distal segments undergo Wallerian degeneration after 12-24h, the lifespan of the explants is limited. However, axonal transport has been shown to remain stable and comparable to *in vivo* measurements in sciatic axons for

at least 2h after transection. After 2h transport rates in proximal parts of intercostal nerves decline, presumably because further cargo-supply is limited (Misgeld, Kerschensteiner et al. 2007, Kerschensteiner, Reuter et al. 2008). Our transport measurements did not exceed 1.5h after sacrificing the animal and should therefore be in the range of stable mitochondrial flux. Indeed, there was no hint for a decline in transport rates during my imaging period (P90 *thy1-MitoCFP*: 5.9 *vs.*6.1 mito/min transported anterogradely and 2.4 *vs.* 2.1 mito/min transported retrogradely in the first half *vs.* second half of the measurements).

Besides offering good imaging conditions, the triangularis sterni muscle constitutes a suitable muscle for studying motor neuron pathology in ALS. Basically all neurites innervating the triangularis sterni muscle are motor axons (Kerschensteiner, Reuter et al. 2008). This is beneficial when studying a disease that affects specifically motor neurons. Confocal analysis revealed that the triangularis sterni muscle was affected by denervation in SOD^{G93A} mice. Compared to lower limb muscles, denervation occurred later in the disease course, but displayed similar morphological features (Marinkovic, Reuter et al. 2012).

Part 1: Mitochondrial transport in motor axons of a SOD^{G93A} mouse model

The first aim of this project was to investigate mitochondrial transport in motor axons from a mouse model of ALS (SOD^{G93A}). I addressed this question, because disrupted transport has been widely implicated in neurodegenerative diseases (Duncan and Goldstein 2006, De Vos, Grierson et al. 2008), especially in ALS (Rothstein 2009), but the central question of whether the temporal and cell biological characteristics of disrupted transport would be compatible with a *causative* role of axonal transport in motor neuron degeneration has not been settled. Indeed, no detailed time course of transport changes and its relationship with motor axon degeneration had been available at the onset of my work (in 2007).

A review of the literature

Several studies already suggested an axonal transport deficit in ALS (Breuer, Lynn et al. 1987, Sasaki and Iwata 1996, Warita, Itoyama et al. 1999, Williamson and Cleveland 1999, Pun, Santos et al. 2006, De Vos, Chapman et al. 2007, Bilsland, Sahai et al. 2010, Vande Velde, McDonald et al. 2011, Magrane, Sahawneh et al. 2012). These studies were based on various technical approaches to investigate axonal transport of proteins or organelles, applied to material derived from ALS patients, different mutant SOD1-based mouse models, as well as on cell culture models. More recently, investigations on TDP-43 proteinopathies implied that

axonal transport defects also contribute to pathogenesis in non-SOD1 based ALS models (Pesiridis, Tripathy et al. 2011). Although the published results are partially contradictory in detail, there is evidence of axonal transport deficits in ALS, which should then emerge early in the disease course.

Most directly relevant to the human disease, but also most limited in material availability and reproducibility, are studies in material derived from human patients. Particle transport in nerve biopsies was measured using intrinsic (differential interference) contrast. This data suggested an increase in mean anterograde speed, whereas retrograde velocity and traffic density appeared to be decreased (Breuer, Lynn et al. 1987). Unfortunately, these studies predated the availability of organelle specific labels (such as vital dyes that selectively label mitochondria; (Haass-Mannle and Zimmermann 1997) - hence the exact nature of the affected organelles remained unclear. Moreover, these studies could only involve symptomatic patients and were based on small tissue biopsies, so that a direct correlation between the observed transport changes, disease stage and axon or synapse pathology was not possible. Further, albeit indirect, hints for axonal transport deficits in human ALS came from histological studies. Ultrastructural investigations of proximal axon segments from ALS patients revealed accumulation of mitochondria and other organelles (Sasaki and Iwata 1996). These observations were corroborated by observations in mouse models of ALS (Collard, Cote et al. 1995). For examples, Pun et al. found a subset of NMJs depleted from synaptic vesicles in SOD^{G93A} mice at P35-P38, which was interpreted as sign of reduced provision of organelles (Pun, Santos et al. 2006). Similarly, sciatic nerve ligation combined with immunohistochemical analysis revealed altered rates of accumulation of kinesin and dynein on both sides of the ligation site in SOD^{G93A} mice. Presymptomatic animals showed a selective decrease of kinesin accumulation, whereas with onset of symptoms a reduction of immunoreactivity for both kinesin and dynein was found. These data implied impaired axonal transport primarily in anterograde direction (Warita, Itoyama et al. 1999). In a similar experiment, another group found a more profound reduction of retrograde transport compared to anterograde transport, which affected neurotrophic and growth factors (Perlson, Jeong et al. 2009). Furthermore, anterograde transport of radioactively labeled cytoskeleton proteins (slow axonal transport, SAT) in SOD^{G37R} and SOD^{G85R} mice was slowed months before the onset of clinical symptoms. This slowing was cargo-specific, and some proteins were affected earlier than others. In the same study, no changes were found for fast axonal transport (FAT) of proteins (Williamson and Cleveland 1999). Similar observations came from another mouse model of ALS. Overexpression of the human neurofilament heavy-subunit gene (*NF-H*) also resulted in reduced SAT rates for cytoskeleton proteins (Collard, Cote et al. 1995). In a SOD^{G93A} mouse line with reduced copy

number and delayed onset of the disease, SAT of proteins was found considerably reduced by the time mice exhibited muscle weakness (around P200). At the same age slowing of FAT was variable and protein-specific. At P150 neither SAT nor FAT appeared to be reduced (Zhang, Tu et al. 1997). Several studies showed reduced retrograde transport rates of tetanus toxin fragments in *SOD^{G93A}* motor neurons. In vivo imaging of single axons showed significant slowing of retrograde transport of tetanus-toxin-labeled vesicles at P36. The deficit worsened with disease progression and could not be detected in motor neurons at P25 or in sensory axons (Bilsland, Sahai et al. 2010). Comparing motor neuron cultures from *SOD^{G93A}* and littermate control embryos, fewer and slower transport of tetanus-toxin-labeled vesicles was found (Kieran, Hafezparast et al. 2005). In motor neuron cultures from *SOD^{G93A}* embryos, mitochondrial transport was reduced selectively in anterograde direction, whereas the amount of retrograde transport appeared to be increased. Mitochondrial velocity was reduced only in anterograde direction. Transport of membrane-bound organelles (e.g. synaptic vesicles), in contrast, was reduced in anterograde and retrograde direction (De Vos, Chapman et al. 2007). Most relevant to my study, mitochondrial transport in sciatic nerves from *SOD^{G93A}, thy1-MitoCFP* mice *in vivo* was found to be slowed in anterograde and retrograde directions at presymptomatic stages. In this study, which was published after I finished my own measurements, alterations neither in the frequency of moving mitochondria nor in the proportion of anterograde to retrograde transport were detected at P36 (Bilsland, Sahai et al. 2010).

In conclusion, there is evidence in the literature that axonal transport deficits emerge early in ALS models and are potentially cargo- and direction-specific. Differences between various SOD1 mouse lines or between the *in vivo* and *in vitro* situations remain possible and might explain some of the conflicting findings. It is not clear how transport deficits correlate with onset and progression of degeneration of motor neurons and if they contribute to pathogenesis in ALS.

Mitochondrial transport in motor axons of murine ALS models: My own results

As discussed in the previous section, the literature supports the idea that axonal transport deficits exist in ALS and its mouse models. Indeed, numerous reviews ascribe a central pathogenic role to such transport deficits (Boillee, Vande Velde et al. 2006, Chevalier-Larsen and Holzbaur 2006, De Vos, Grierson et al. 2008, Magrane and Manfredi 2009, Rothstein 2009). However, the exact nature of the transport deficit (e.g. which organelles or which directions of transport are affected) is controversial, in part due to the heterogeneity of the

methods, disease models and metrics used to quantify axonal transport. This thesis represents the attempt (or at least its beginning) to definitively characterize transport of one organelle, mitochondria, by *ex vivo* measurements throughout the disease course of the most widely used ALS model, the *SOD^{G93A}* mouse. Mitochondrial transport was recorded by performing time-lapse imaging with high temporal resolution (image acquisition rate of 1/sec) in living *SOD^{G93A}* motor axons. The experimental set-up allowed quantitative analysis and establishment of a chronological sequence of transport deficits for both anterograde and retrograde direction.

My results showed a profound reduction in mitochondrial flux in *SOD^{G93A}, thy1-MitoCFP* mice months before symptoms or neuromuscular denervation appeared (NMJ denervation in the triangularis sterni muscle became obvious after P90). The transport deficit affected both anterograde and retrograde direction. Anterograde transport was significantly reduced at P20, whereas statistically significant differences in retrograde transport could first be detected around P60. These results on flux differed from results published by another group in parallel to my work (Bilsland, Sahai et al. 2010), but were consistent with other results previously obtained in cell culture (De Vos, Chapman et al. 2007). I will discuss possible explanations for this discrepancy below. My results on single-organelle movement characteristics (speed, pausing behaviour, etc.) were consistent with previously reported changes: The average velocity of moving mitochondria was reduced. This slowing originated from a higher frequency of pauses, an increase in the frequency of intermediate velocities and a reduction in maximum velocity.

In addition to transport rates and single-organelle movement characteristics, my study yielded information about the variability from axon to axon over the disease course and about mitochondrial morphology: *(1)* Analysis of *transport on the level of individual axons* revealed heterogeneity within *SOD^{G93A}* axons, with some axons apparently not affected by the transport deficit. This might mean that a subset of axons was resistant to *SOD^{G93A}*-induced pathology (Frey, Schneider et al. 2000). However, it cannot be excluded that our measurements included a small proportion of sensory axons with normal transport rates. This would result in an underestimation of the actual deficit in motor neurons. *(2) Mitochondrial morphology* in *SOD^{G93A}, thy1-MitoCFP* intercostal motor axons was altered. Mitochondria were shorter and rounder than in control animals. This finding was similar to histopathological observations of anterior horn cells in ALS patients (Hirano, Donnenfeld et al. 1984, Hirano, Nakano et al. 1984, Sasaki and Iwata 2007). These morphologic changes could not be detected in axons innervating extra-ocular muscles, which are also otherwise spared in ALS. This finding

suggested a correlation between mitochondrial morphology and axon degeneration, and would be compatible with a causative role of mitochondrial changes in motor axon degeneration.

My results in the context of the literature and in light of subsequent studies in our group

Studies by other laboratories

Studies by other laboratories support the idea that axonal transport deficits emerge early in ALS models. However, some of the results (e.g. which organelles or which directions of transport are affected) are controversial. Heterogeneity of the methods, disease models and analyzed parameters might explain some of the conflicting findings. I will discuss these aspects in the subsequent section. In this part of my discussion I concentrate on studies that analyzed mitochondrial transport in *SOD^{G93A}* disease models.

De Vos et al. found that the fraction of motile mitochondria was unaltered in *SOD^{G93A}* motor neuron cultures, with a deficit in anterograde and an increase in retrograde transport (De Vos, Chapman et al. 2007). Velocity of moving mitochondria was described to be reduced only in anterograde direction. In my *ex vivo* experiments in *SOD^{G93A}, thy1-MitoCFP* mice, anterograde transport appeared to be reduced earlier in the disease course than retrograde transport. Later, transport was reduced in both directions. For cultured motor neurons it is problematic to determine the exact corresponding stage in a disease course. *SOD^{G93A}* motor neuron cultures used by De Vos et al. might correspond to an early stage in the disease, with a reduction in anterograde but not yet in retrograde transport. In addition, as discussed above, there is evidence that axonal transport in vitro differs from transport in vivo or in explants. The differences in transport properties may result from altered myelination of neurons in cell culture (Bilsland, Sahai et al. 2010), as myelination can influence axoplasmic Ca^{++} levels and microtubule stability and therefore axonal transport parameters (Kirkpatrick and Brady 1994, Kiryu-Seo, Ohno et al. 2010).

In parallel to our study, Bilsland et al. investigated mitochondrial transport in sciatic nerves from living *SOD^{G93A}, thy1-MitoCFP* mice (Bilsland, Sahai et al. 2010). They found alterations in mitochondrial velocity at presymptomatical stages (P36), with slowed transport in both anterograde and retrograde direction, consistent with our results. However, velocities published by the other group were significantly lower than velocity measurements in this thesis. Also inconsistent with our results, no alterations in mitochondrial flux were detected in

SOD^{G93A} mice at an age of P36. Such discrepancies could result from methodological differences, for example in *(1)* the *experimental set-up* or *(2)* the *imaging protocol*.

(1) Experimental set-up: Bilsland at al. performed transport measurements in sciatic nerves *in vivo*, whereas our study was implemented in intercostal nerves of acute explants (*ex vivo*). It is of course possible, that different nerves are variably affected by mitochondrial transport deficits. If we considered an association with axon degeneration, it would be unlikely that intercostal nerves were affected earlier by a transport deficit than sciatic nerves, as medial and lateral gastrocnemius muscles are denervated earlier than triangularis sterni muscles (Frey, Schneider et al. 2000, Marinkovic, Reuter et al. 2012). Besides, in acute explants of tibialis anterior nerves from 120 day old *SOD*^{G93A} mice, the transport deficit was similar to that in intercostal nerves (Marinkovic, Reuter et al. 2012). On the other hand, it is possible that transport *in vivo* differs from transport in acute explants; although previous studies did not find such deviations (Kerschensteiner, Reuter et al. 2008). We cannot exclude that there are mechanisms, which reduce transport only in explants from *SOD*^{G93A} mice and not *in vivo*. However, time-lapse imaging *in vivo* has more disruptive factors, which reduce data quality (e.g. muscular movements, pulse, respiration, less superficial axons). Reduced data quality could result in an overall lower number of quantifiable mitochondria, and impede the detection of transport differences.

(2) Imaging protocols: Different results may also come from different imaging protocols. Bilsland et al. performed time-lapse confocal microscopy with an image acquisition rate of 1 frame every 5-8 seconds (Bilsland, Sahai et al. 2010). For this thesis I performed time-lapse epifluorescence microscopy with an image acquisition rate of 1 frame every second. Confocal microscopy generally features high optical resolution, as light from out-of-focus-planes is eliminated by a pinhole that acts as a spatial filter. However, fluorescent objects from planes under and above the plane in-focus are missed. In addition, as much of the light intensity is blocked by the pinhole, longer light exposure is often required, with the risk of increased phototoxicity. Epifluorescence microscopy typically displays lower optical resolution and more background fluorescence because out-of-focus fluorescence reaches the detector. While this lack of optical sectioning increases background, it also allows detection of fluorescent objects that are slightly out-of-focus and usage of relatively low light levels with little phototoxicity. In addition, our image acquisition rates are at least 5-fold higher than those from the study by Bilsland et al., making it easier to track moving objects. To sum up, it is plausible that the combination of epifluorescence microscopy and higher image acquisition rates allows

detection of more moving objects and results in more precise quantification. Values for peak velocities should also be more precise, as there is less averaging.

A study by Zhu et al. addressed the functional importance of mitochondrial transport deficits in *SOD^{G93A}* mice. They showed that depletion of the mitochondrial docking receptor syntaphilin increased mitochondrial motility by a factor of 2 and artificially rescued a transport deficit in *SOD^{G93A}* mice. However, it neither affected onset of symptoms or life-span nor did it affect histological findings on motor neuron degeneration. These findings question a critical role of the mitochondrial transport deficit in motor neuron pathology. The authors suggested that deficient transport of cargoes other than mitochondria or mitochondrial dysfunction might play a more important pathogenic role (Zhu and Sheng 2011).

Follow-up studies in our laboratory: Comparison of different nerves, SOD1 lines and multiple cargoes

Analyses of other nerves, cargoes and SOD1 mouse lines were performed by my colleague Petar Marinkovic (Marinkovic, Reuter et al. 2012), on the basis of the results that I obtained during my thesis work. First, he showed that in the *SOD^{G93A}* line, mitochondrial transport was also reduced in isolated tibialis nerves (which innervate the gastrocnemius muscle) but not in sensory saphenous nerves. In *SOD^{G93A}* intercostal nerves, retrograde transport of Cholera Toxin Subunit B (CTB)-labeled vesicles was reduced similarly to mitochondrial transport. In further analyses, P. Marinkovic showed that different SOD1 mouse lines with similar motor neuron disease phenotypes differ in their mitochondrial transport parameters. The *SOD^{G37R}* line, which expresses an enzymatically active form of the protein (so does *SOD^{G93A}*), displayed a transport deficit at presymptomatical disease stages, similar to my results in the *SOD^{G93A}* line. *SOD^{G85R}* mice express an unstable and probably enzymatically inactive form of mutant SOD1 and display first symptoms at approximately 9 months of age. In this mouse line, mitochondrial flux in both anterograde and retrograde direction was normal even in preterminal stages of the disease (10% loss of body weight), when other axons of the same nerve were already fragmented. The same was true for retrograde transport of CTB-labeled vesicles. Otherwise, in *SOD^{WT}* mice (overexpressing human wild-type SOD1) profound transport deficits were apparent 2 months after birth but did not cause axon degeneration (apart from mild denervation at 12 months of age). In sum, transport deficits were neither necessary nor sufficient to cause axon degeneration. The findings dissociated transport deficits from neurodegeneration and SOD1 mutations from transport deficits. Mitochondrial shape abnormalities were also apparent in the *SOD^{G93A}*, *SOD^{G37R}* and *SOD^{WT}* lines, but not in the

SOD^{G85R} line. In summary, transport deficits and altered mitochondrial morphology were found in mouse lines that overexpress SOD1 with preserved enzymatic activity but not in those lines with inactive mutants. Which parameters in the end influence the transport deficit (e.g. enzymatic activity, protein expression levels, subcellular localization, aggregation state etc.) could not be definitely differentiated from the study by Marinkovic et al. (Marinkovic, Reuter et al. 2012).

Axonal transport as a possible pathogenic mechanism in SOD1-mutants

The mechanisms by which mutant SOD1 induces selective motor neuron death are not properly understood. Although transport disruptions could not be found in all SOD1 lines, a disruption of axonal transport would theoretically be a suitable pathological mechanism in motor neuron diseases: *(1)* Transport disruptions provide an explanation for the *cellular selectivity* of the disease. Motor neurons with their long processes are particularly dependent on efficient transport of organelles, proteins, and molecules and would be vulnerable to a transport deficit (Collard, Cote et al. 1995). *(2)* The *'die-back' model* of many motor neuron diseases is consistent with shortage in energy or other resources in the periphery. This shortage could be a consequence of reduced transport towards the synapse. *(3) Onset* of most motor neuron diseases is in adulthood. Retardation of slow axonal transport has been found during normal aging, and might contribute to a disease-evoked transport deficit (McQuarrie, Brady et al. 1989). *(4) Mutations in genes* associated with axonal transport were described in patients with ALS and other neurodegenerative disorders (Duncan and Goldstein 2006). Transgenic mice with deficits in retrograde transport exhibit progressive motor neuron degeneration (Hafezparast, Klocke et al. 2003). *(5) Ultrastructural analyses* of motor axons from mouse models with motor neuron disease showed organelle accumulations and revealed indirect hints for transport disruptions, such as reduced organelle densities in the periphery (Boillee, Vande Velde et al. 2006, Shan, Chiang et al. 2010). *(6)* Misfolded wild-type SOD1 is found in spinal cord tissue from patients with sporadic ALS, and was shown to inhibit kinesin-based fast axonal transport in isolated squid axoplasm. Disturbed transport could therefore constitute a *common pathogenic pathway* in both SOD1 mutation-based and sporadic ALS cases (Bosco, Morfini et al. 2010).

There are several hypotheses about how SOD1 mutations could cause axonal transport deficits. Possible mechanisms include alterations of *(1) cargoes* (here, mitochondria), *(2) energy-supply* (ATP), *(3) motor proteins and associated molecules* or *(4) cytoskeletal tracks and cytoskeleton-associated proteins* (De Vos, Grierson et al. 2008).

(1), (2) Mitochondrial alterations: Mitochondrial alterations could influence transport in their roles as a cargo of transport, as Ca^{++}- buffering organelles or as ATP providers.

Alterations in mitochondrial morphology in early-stage degenerating motor neurons of ALS patients were shown by histopathological studies (Hirano, Donnenfeld et al. 1984, Hirano, Nakano et al. 1984, Sasaki and Iwata 2007). These alterations were also found in several transgenic SOD1 mouse models (SOD^{G93A}, SOD^{G37R}) (Wong, Pardo et al. 1995, Higgins, Jung et al. 2003) and resulted from massive mitochondrial vacuolation with expansion of the intermembrane space. However, morphological changes could not be detected in other bona fide ALS models (SOD^{G85R}). Indeed, in transgenic mice, mitochondrial vacuolation appeared to be limited to lines that overexpress active forms of SOD1, and coincided with deficiency in mitochondrial transport (Marinkovic, Reuter et al. 2012). In addition to morphological alterations, reduced density of mitochondria was observed in motor axons from SOD^{G93A} animal models (De Vos, Chapman et al. 2007, Marinkovic, Reuter et al. 2012).

There is also evidence for functional deficits of mitochondria in motor neuron diseases. Alterations in electron transport chain function were reported from studies with human ALS patients, animal models and cell cultures. Although some of the results are controversial, several studies showed a biochemical defect or reduced membrane potential in neuronal mitochondria from ALS models (Bowling, Schulz et al. 1993, Jung, Higgins et al. 2002, Mattiazzi, D'Aurelio et al. 2002, Boillee, Vande Velde et al. 2006, De Vos, Chapman et al. 2007). A study by Miller et al. showed that in wild-type neuronal cell cultures, the direction of mitochondrial transport correlated with its potential. Anterogradely transported mitochondria tended to have a higher membrane potential than retrogradely transported ones (Miller and Sheetz 2004). A possible explanation is that retrogradely transported mitochondria were merely on average older. On the other hand, if reduced membrane potential was a cause for retrograde transport, biochemical function defects could explain the transport pattern we observed in young SOD^{G93A} mice.

Mitochondrial depletion and damage could both diminish ATP supply, and therefore adversely affect the energy-consuming movement of motor proteins along microtubules. In addition, mitochondria have important functions as Ca^{++} buffers (Bacman, Bradley et al. 2006). Mitochondrial depletion or impaired function goes along with reduced Ca^{++}- buffering capacity. Proteins associated with mitochondrial transport (such as Miro) are dependent on the Ca^{++} concentration in the cell. Elevated cytosolic Ca^{++} levels were found in neuronal cell cultures from SOD^{G93A} mice (Tradewell, Cooper et al. 2011) and could be capable of arresting

microtubule-based mitochondrial movement, potentially resulting in a vicious cycle (Goldstein, Wang et al. 2008).

(3) Motors and associated proteins: Motor protein function could be disturbed directly in SOD1-mutants. For example, mutant SOD1 was shown to co-localize and interact with dynein, the major motor protein for retrograde transport. It is not clear whether this interaction inhibits dynein function, but it is a possible mechanism how mutant SOD1 could contribute to a defect in retrograde transport (Zhang, Strom et al. 2007, De Vos, Grierson et al. 2008, Magrane, Sahawneh et al. 2012). Humans and transgenic mice expressing mutant forms of dynactin or dynein develop motor neuron disorders (LaMonte, Wallace et al. 2002, Hafezparast, Klocke et al. 2003, Puls, Jonnakuty et al. 2003). However, *Loa*-mice (carrying a mutation in the dynein heavy chain) crossed with SOD^{G93A} mice resulted in an unexpected phenotype. Rather than accelerating motor neuron degeneration, the presence of both mutant proteins was protective. The mechanisms underlying this effect are not clear; one possibility is that the dynein mutation counterbalances an inhibition in anterograde transport, so that more mitochondria remain in the axons (Kieran, Hafezparast et al. 2005).

On the other hand, motor protein function could be affected indirectly, through modifications in line with altered intracellular signalling pathways. Mutant SOD1 appears to result in pathogenic signalling that influences phosphorylation of molecular motors and cargoes. Through such pathways, other cell types might contribute to ALS pathology (e.g. microglia and astrocytes). One hypothesis is that astrocytes influence the motor neuronal phenotype by secretion of inflammatory signals such as TNF-α (Julien 2007, Nagai, Re et al. 2007). Inflammatory or other signals could inhibit kinesin function, e.g. via p38 MAPK-dependent phosphorylation (De Vos, Grierson et al. 2008).

(4) Cytoskeleton and associated proteins: One early pathological hallmark in motor axons of SOD1 mice is the accumulation of hyperphosphorylated neurofilaments (De Vos, Grierson et al. 2008). Modulation of the neurofilament gene expression pattern, in terms of deletion of neurofilaments or overexpression of the heavy chain, had a protective effect on motor neurons expressing mutant SOD1 (Couillard-Despres, Zhu et al. 1998, Williamson, Bruijn et al. 1998). Besides providing structural stability, neurofilaments could affect function of microtubules and actin filaments, which constitute the tracks for axonal transport (Julien and Mushynski 1998). It is also plausible that aggregations of neurofilaments or other proteins impair axonal transport by physical blockage (Bacman, Bradley et al. 2006).

Deficits in mitochondrial transport might arise from reduction or alterations of cytoskeletal tracks, presumably microtubules. Fanara et al. described hyperdynamic microtubules in *SOD*^{G93A} motor neurons. Treatment with a microtubule-modifying agent (noscapine) delayed disease onset and extended survival in this mouse model (Fanara, Banerjee et al. 2007). Disruption of microtubules in neuronal cell cultures by vinblastine treatment resulted in reduced number of mitochondria entering the axon, a net increase in retrograde transport rates and decreased average and maximum velocities (Morris and Hollenbeck 1995). Transport properties in *SOD*^{G93A} motor axons resembled those of microtubule-depleted neurons. This indicates that mutant SOD1 could cause transport deficits via reduction or modification of microtubular tracks or microtubule-associated proteins.

Conclusions - Part 1

In the *SOD*^{G93A} mouse line I found profound transport deficits months before neurodegeneration occurs. This was so far one of the earliest alterations observed in models for motor neuron disease. The transport deficit was limited to motor neurons and could not be detected in sensory neurons (studies in sensory neurons were performed by P. Marinkovic) (Marinkovic, Reuter et al. 2012). Thus, in *SOD*^{G93A} mice transport disruptions were actually present, and would fulfil some of the tenets of neurodegeneration-causing mechanisms (e.g. onset before axon loss, motor neuron specificity). On the other hand, my results showed that transport disruptions did not immediately lead to neurodegeneration, as axons could survive several months with severe transport deficits. Apparently neurons have a 'reserve capacity' in their normal organelle supply, so that they can survive for months with considerably reduced axonal transport. In addition, the decrease in retrograde transport could compensate in part for the deficit in anterograde transport, even though my data did show a reduced net translocation (anterograde minus retrograde transport).

The follow-up studies by my colleague P. Marinkovic on the *SOD*^{G85R} and *SOD*^{WT} mice further dissociated transport changes from neurodegeneration, as degeneration could occur in the absence of a transport deficit and in converse, a transport deficit did not necessarily lead to neurodegeneration. This is an argument against the hypothesis that transport disruptions alone could be the primary causative mechanism in SOD1-based ALS models (Marinkovic, Reuter et al. 2012). Furthermore, the fact that artificially increasing mitochondrial mobility did not delay onset or progression of the disease also argues against a decisive role of transport disruptions alone (Zhu and Sheng 2011). Although a primary causative role seems unlikely, motor neuron-specific transport deficits could still contribute to pathogenesis and especially

phenotypic variations between different SOD1 lines (Marinkovic, Reuter et al. 2012). Especially the role of slow axonal transport has not been investigated in my study.

In conclusion, axonal transport deficits occurred in presymptomatic *SOD^{G93A}* mouse models, and might also be apparent in other motor neuron diseases. As this change was found earlier than any other parameters, it could serve as a presymptomatic biomarker, even though it might not be a predictor of neurodegeneration. Imaging axonal transport non-invasively by using manganese tracers and magnetic resonance imaging or kinetic biomarkers in the cerebrospinal fluid could provide new diagnostic options (Minoshima and Cross 2008, Fanara, Wong et al. 2012, Marinkovic, Reuter et al. 2012).

Contrariwise, analyses of other SOD1-mutants revealed heterogeneity of transport deficits among mouse models with different mutations in the same gene. This puts into question if there is one pathogenic mechanism for the disease amyotrophic lateral sclerosis. It appears possible that the disease is pathogenically heterogeneous, and that there are different events that all lead to a phenotype of motor neuron degeneration. On the other hand, part of the pathology in SOD1-based mouse models could be artefacts due to overexpression of the mutated protein. At the moment, it remains questionable whether modulating transport would be a beneficial intervention in motor neuron diseases. Further studies will be required to address this question, preferentially in improved animal models of the disease. In any case, whether axonal transport as a fundamental cell biological process, represents a "translatable" target at all, remains to be seen. Independently of the benefit in ALS therapy, many other neurodegenerative diseases are probably accelerated by transport deficits - so preventing this cell biological decline in neurons remains a desirable, if - as of now - elusive goal.

However, the SOD1-based ALS model is certainly not sufficient to study all aspects of the disease amyotrophic lateral sclerosis. The genetic heterogeneity in human patients with the disease points towards the need to study different disease models. Clarifying the role of axonal transport in die-back motor neuron disorders necessitates investigation of several animal models and possibly also human ALS patients. Transgenic mice that overexpress mutant or wild-type TDP-43 protein are a relatively recent model for a motor neuron disease phenotype comparable to ALS (Wegorzewska, Bell et al. 2009, Wils, Kleinberger et al. 2010). These mice require more detailed functional characterization, also in terms of axonal transport deficits. Indeed, fragments of TDP-43 protein appeared to aggregate when retrograde microtubule-based transport was disrupted (Pesiridis, Tripathy et al. 2011). Promising future disease models would also be SOD1 knock-in mice (as the insertion-site might influence the

phenotype). In conclusion, new animal models for motor neuron diseases need to be established and functionally characterized.

Part 2: Mitochondrial transport in the development of the neuromuscular junction

The second part of my thesis investigated the presence of transport changes in dismantling branches during postnatal development of the NMJ. I addressed this question to explore to what degree disease-related and developmental axon loss might share cell biological mechanisms. Moreover, "resource distribution" has been implicated in regulated axon branch elimination (Barber and Lichtman 1999, Keller-Peck, Walsh et al. 2001, Walsh and Lichtman 2003), and axonal transport could be a means to mediate this resource distribution - an idea that to this date has not been tested experimentally.

A review of the literature

The phenomenon of developmental synapse elimination has been studied for more than 30 years. There are several models of the mechanisms and regulating factors that mediate axon branch loss.

D. A. Riley studied multiple- to single-innervation at developing neuromuscular junctions morphologically using silver stains of rat soleus muscle. He found that retreating axon branches ended in swollen tips (‘retraction bulbs’) and hypothesized that synapse elimination was mostly characterized by complete reabsorption of the process by the parent axon. At least a fraction of axonal content might therefore be actively ‘evacuated’, e.g. by loss of anterograde and/or increased retrograde transport (Riley 1977, Riley 1981). However, this author also suggested that a small subset of branches could undergo fragmentation and Schwann cell phagocytosis. Riley described that multiply innervated NMJs were often characterized by one normal looking axon and accompanying axons that were thinner and showed local swellings (Riley 1977, Riley 1981). More recent morphological studies by Keller-Peck et al. allowed reconstruction of complete motor units and showed that within a single neuron retracting axon branches withdrew asynchronously and were distributed throughout the axonal arbor (Keller-Peck, Walsh et al. 2001). These authors found no evidence that branches with more proximal or distal origin were different in terms of progress toward single-innervation. In addition, there was no obvious correlation regarding the elimination stage (receptor occupation) of branches originating from the same branch-point. The authors suggested that local factors regulate synapse elimination rather than the soma orchestrating

its arbors' competitions. What factors determine the local competitive vigor of axon branches remained unclear (Keller-Peck, Walsh et al. 2001). Another finding of this study was a linear correlation between axon branch diameter and territory occupied by the corresponding NMJ. *In vivo* imaging revealed that thin, atrophic axon branches that innervated small territories often retracted within the next 24 hours (Keller-Peck, Walsh et al. 2001). In addition to this morphological description, numerous studies support the view that competition between converging inputs is influenced by inter-axonal differences in activity levels. Based on mathematical modelling, Barber et al. suggested that the total amount of neurotransmitter release is critical, rather than the frequency of release. The elimination of individual axon branches would then result in redistribution of the 'resource' neurotransmitter. In this way, the authors reconciled the opposite observations that *(1)* focal blockade of neurotransmission could cause synapse elimination, suggesting that active axons had a competitive advantage, but on the other hand *(2)* small motor units were generally more active (Barber and Lichtman 1999). *In vivo* imaging of developing NMJs showed that typically at a doubly-innervated synapse, one axon withdrew from the postsynaptic site while the competing axon extended processes and occupied the abandoned sites, therefore expanding its territory. In rare instances the remaining axon did not reoccupy a site (Walsh and Lichtman 2003). These findings indicate that withdrawal of an axon is preceded by a coordinated process that includes stepwise diminishment and expansion of the competitors, which could be promoted by intrinsic dynamism of young axons (Turney and Lichtman 2012). Synaptic takeover could result in greater neurotransmitter release and increased synaptic strength. However, the relative amount of territory was not in all cases a reliable predictor of the final outcome. The authors concluded that simultaneously proceeding competitions within the same neuron could influence the availability of a resource and therefore result in unexpected 'flip-flops' (Walsh and Lichtman 2003). Bishop et al. further characterized ultrastructural details in axon branch retraction to explore the mechanisms underlying branch dismantling. They found that at least a fraction of an axon branch's material was shed as membrane-enclosed 'axosomes'. These axosomes were enveloped by Schwann cells, suggesting an interaction between axons and glial cells during the elimination process (Bishop, Misgeld et al. 2004). 'Axosome-shedding' was recognized as a contributor to axon removal and synaptic segregation. Electron microscopy studies showed that axon branches undergoing elimination had reduced numbers of disarrayed microtubular tracks (Bishop, Misgeld et al. 2004). Song et al. found that developmental synapse elimination was associated with increased lysosomal activity. This finding is consistent with digestive mechanisms such as autophagy and heterophagy (Song, Misgeld et al. 2008). In parallel to my work, Liu et al. studied axonal transport during synapse

elimination in Drosophila. They showed that in dismantling branches synaptic vesicles were retrogradely transported into the innervating axon. When retrograde transport was disrupted, presynaptic elimination appeared delayed. The authors concluded that in flies retrograde transport was required for presynaptic elimination (Liu, Chen et al. 2010). It should be noted, however, that 'synapse elimination' in flies represents a non-competitive remodelling process that contributes to axon-muscle matching, a process that has no simple equivalent in vertebrates. Invertebrates lack true homologues of the competitive remodelling processes characteristic of vertebrate neurodevelopment ((Lichtman and Colman 2000); discussion, see below).

Mitochondrial transport in the development of the neuromuscular junction: My own results

Several arguments from the literature support the idea of resource distribution as a mediator in axonal competition - but 'resource distribution' remained an abstract concept without cell biological correlate. This was due to previous methodological limitations that did not allow direct observation and quantification of transport at the level of individual axon branches within their natural environment. Our approach, which took advantage of transgenic mice with fluorescently labeled cells and organelles, overcomes these limitations. My work was aimed to measure mitochondrial transport during the transition from multiple- to single-innervation at the NMJ. To address this issue, I performed time-lapse imaging of terminal motor axon branches and categorized them according to their developmental stage (refer to section 'Material and Methods, Time-lapse analysis').

My results showed a profound reduction of both anterograde and retrograde mitochondrial transport within axon branches that were currently undergoing elimination and ended in a retraction bulb. Nevertheless, even in those branches transport was not completely absent. A reduction in transport was already apparent in morphologically atrophic axon branches that were likely to undergo elimination but had not yet lost contact to the muscle fiber. Axon branches that had successfully competed against other inputs resulting in a singly innervated muscle fiber, as well as putative ‘winner’ branches in doubly innervated NMJs, had increased transport, compared to branches that were still engaged in competitions with open outcome. Consequently, one NMJ appeared to receive a constant number of mitochondria, irrespective of whether it was innervated by one or two axon branches. This was on the one hand intuitive; as during the elimination period neither the number of NMJs, nor the number of motor neurons (Sanes and Lichtman 1999), nor the amount of transport in proximal motor axons changes (Misgeld, Kerschensteiner et al. 2007). On the other hand, this result indicated

that the amount of transport could be regulated locally on the level of individual axon branches, an unexpected and unprecedented example of an axon's capability of local homeostatic regulation.

It is known from previous studies, that thin axon branches often innervate small territories and soon retract from the muscle fiber (Keller-Peck, Walsh et al. 2001). Although I could not prove a predictive role of local transport deficits in axon branch retraction, such mechanisms appear plausible, as I found significant correlation of mitochondrial transport with axon diameter in doubly innervated NMJs.

Retreating axons did not show increased retrograde transport rates. This refutes the hypothesis that a major fraction of axonal content is retracted towards the persisting axon (Riley 1977, Riley 1981), and sets mammalian synapse elimination farther apart from NMJ remodelling in flies (Liu, Chen et al. 2010). In contrast, our observations were consistent with the theory that axonal content is eliminated by auto- or hetero-digestive mechanisms (e.g. digestion by surrounding Schwann cells) (Bishop, Misgeld et al. 2004).

My results in the context of the literature and in light of subsequent studies in our group

Studies by other laboratories

As mentioned before remodelling (and 'synapse elimination') also occurs during the development of the NMJ in Drosophila. In parallel to my work, Liu et al. studied axonal transport during synapse elimination in fruit flies. In dismantling branches, synaptic vesicles were retrogradely transported into the innervating axon. When retrograde transport was disrupted, presynaptic elimination appeared delayed (Liu, Chen et al. 2010). The authors concluded that in flies retrograde transport was required for presynaptic elimination. They hypothesized that retrogradely transported synaptic constituents might be reused for persisting synaptic connections (Liu, Chen et al. 2010). Those findings are not consistent with our observations of mitochondrial transport in murine synapse elimination. My results indicated that both anterograde and retrograde mitochondrial transport were reduced in retreating axon branches. On the one hand, those disparities might be derived from the observation of different organelles. On the other hand, it is possible that neuromuscular synapse elimination is mechanistically different in mice and Drosophila. In fact, there are several hints that synapse elimination in Drosophila and mammals cannot be compared that easily. For example, in Drosophila (in contrast to the findings in mice) there is no evidence for the formation of retraction bulbs or an involvement of glial cells during neuromuscular

synapse elimination (Liu, Chen et al. 2010), indicating that there might also be differences in the role of axonal transport. More fundamentally, synapse elimination at the fly NMJ is not a competitive process between several motor axons. Still, it would be interesting to investigate whether defects in retrograde transport would affect neuromuscular synapse elimination in mice - an experiment that to my knowledge has not been done, but for which the necessary tools are now available.

Follow-up studies in our laboratory: Correlation of transport with territory, branch-point studies, functional investigations on microtubules

Subsequent studies based on my results performed by Monika Brill in our lab, addressed the question whether there is a correlation of mitochondrial transport and the postsynaptic territory an axon branch occupied. As the territories of two competing axon branches are highly intermingled, the proportion each axon innervates cannot be easily distinguished in *thy1-YFP*[16] mice. M. Brill measured transport in axon branches from doubly innervated NMJs and afterwards bleached one branch under a confocal microscope by parking the diffraction-limited laser on one of the inputs (Brill, Lichtman et al. 2011). As the fluorescent protein from the presynaptic region constantly diffuses into the axon, the entire input gets bleached and its territory can be differentiated from the territory held by the competing branch. Monika Brill found a strong correlation between both anterograde and retrograde transport and the territory of the respective branch, but at the same time also a 'cut off' size, below which a branch tended to have very little transport, despite still innervating up to 20% of a NMJ. When she plotted net transport (anterograde minus retrograde) against the territory, she further found that net transport was disproportionately low in branches that occupied 21-40% of the territory. These results indicated that net transport was excessively reduced before substantial withdrawal from the muscle fiber (unpublished data).

A further experiment performed by M. Brill addressed the question whether transport in 'winner' branches was influenced by the developmental stage of their neighbouring axons. She measured transport at terminal branch-points, with one branch going to a singly innervated NMJ and the other branch either *(1)* ending in a retraction bulb, or *(2)* going to a doubly innervated NMJ, or *(3)* going to a singly innervated NMJ. M. Brill found that transport in winner branches next to retreating branches was significantly higher, compared to winner branches sharing a terminal branch-point with other successful branches. If resource distribution contributes to competitiveness, losing axon branches should indeed convey an advantage for

ongoing and upcoming neighbouring competitions (unpublished data). Interestingly this provides a rather local means of 'resource distribution' within an arbor.

A further open question that derived from my results was which mechanisms might explain the lack of transport in dismantling (or 'losing') branches. One leading hypothesis based on the results of Bishop et al. (Bishop, Misgeld et al., 2004) was early dismantling of microtubules. Tatjana Kleele in the lab established transgenic mice with fluorescently labeled microtubule caps, which act as an indicator for the stability of microtubules. She found that branches occupying larger territories had more stable microtubules. Branches ending in retraction bulbs had very unstable microtubules. Unstable microtubules could be the reason for reductions in axonal transport (unpublished data).

Axonal transport as a possible regulatory mechanism in developmental synapse elimination

There are several reasons why I investigated mitochondrial transport as a putative factor to regulate local axon branch elimination. *(1)* Retreating branches show particular *morphologic changes*, like thinning and local swellings, which have long been interpreted as signs of local atrophy and possibly starvation (Riley 1977, Keller-Peck, Walsh et al. 2001). *(2)* In contrast to most neurodegenerative diseases, developmental axon branch elimination is a *local phenomenon*, since each motor neuron wins some of its competitions while losing others (Kasthuri and Lichtman 2003). The distribution of resources could be regulated locally, e.g. at a branch-point (Barber and Lichtman 1999, Kasthuri and Lichtman 2003). Reduced anterograde transport could lead to depletion of such resources, like nutrients, neurotransmitters and organelles and thus promote elimination of the respective branch (Buffelli, Burgess et al. 2003). At the same time, other branches of the same neuron would benefit from the redistribution. *(3) Electron microscopy studies* showed that axon branches undergoing elimination have reduced numbers of disarrayed microtubules, which display the major tracks for axonal transport (Bishop, Misgeld et al. 2004). *(4)* Deficits in axonal transport are considered to contribute to global axonal dystrophy in many *neurodegenerative diseases* (De Vos, Grierson et al. 2008). Such mechanisms could result from dysregulation of physiologically occurring programs, which might for example be involved in axon dismantling during development. *(5)* One possible candidate as such a resource is the amount of *mitochondria* transported into competing branches. Mitochondria are not distributed randomly, but distribution and transport can be regulated locally (e.g. by focal stimulation with neurotrophic factors, intracellular Ca^{++} concentration, myelination, etc.) (Chada and Hollenbeck 2003, Wang and Schwarz 2009, Ohno, Kidd et al. 2011).

My results were consistent with the idea that mitochondrial transport could be regulated locally on the level of individual axon branches. Possible mechanisms for such transport regulations include *(1) local modification of the cytoskeletal tracks*, *(2) associated proteins* or *(3) local signalling pathways*.

(1) Cytoskeleton: A reduction or modification of microtubules as the major tracks is a conceivable mechanism how transport could be regulated locally. Reduction of microtubule density in retreating branches would result in fewer tracks and possibly less mitochondria entering the axon arbor. An argument for this hypothesis is that retreating axon branches were in average thinner than persisting ones (indicating reduced amount of cytoskeletal proteins, particularly neurofilaments) and that there was statistical correlation between axon branch diameter and transport. Studies performed by T. Kleele indicated that the stability of microtubules was reduced in retreating branches, which could also lead to a reduction in axonal transport along those tracks.

(2) Associated proteins: Amount of transport into axon branches could be regulated by modification of microtubule-associated proteins or motor proteins. Such modifications could be mediated via signals inside the motor axon or released by the environment, e.g. Schwann cells, competing motor axon branches or muscle fibers. In neurodegenerative diseases (like Alzheimer's disease) the microtubule-associated protein tau was found to be hyperphosphorylated. Such phosphorylated forms of the protein could destabilize microtubules and disrupt axonal transport (Cowan, Bossing et al. 2010). It seems plausible that similar protein modifications could also play a role in regulated axon branch elimination during development.

(3) Signalling molecules: Mitochondrial transport and distribution is regulated by a number of factors and signalling pathways. Such factors include, for example, cytosolic Ca^{++} concentration (Wang and Schwarz 2009), activation of NGF receptors (Chada and Hollenbeck 2003), electrical activity and myelination (Ohno, Kidd et al. 2011). To what extend such mechanisms are involved in mitochondrial transport regulation during development has to be further elucidated by subsequent studies.

Conclusions - Part 2

My results showed profound reductions in anterograde and retrograde mitochondrial transport when axon branches retreated from muscle fibers or looked morphologically atrophic. In contrast, persisting branches had increased transport compared to branches in

ongoing competitions. Those results were consistent with the idea that mitochondrial transport could be regulated locally on the level of individual axon branches. A reduction in axonal transport did occur in atrophic and dismantling branches, making it a plausible mechanism to mediate competition between converging inputs. In contrast to the findings in Drosophila (Liu, Chen et al. 2010), my data did not suggest an evacuation of organelles from eliminated branches.

Follow-up studies by M. Brill further supported the idea that net transport was reduced before branches had lost substantial postsynaptic territory. In addition, branch-point studies by M. Brill showed that organelles from losing axon branches were actually rerouted into neighbouring branches. These findings suggested that loss of branches and resulting resource redistributions could indeed influence competitive vigor of nearby branches from the same neuron. Subsequent studies by T. Kleele indicated that microtubule stability was reduced in retreating branches. Diminished stability of the major tracks would be a conceivable mechanism of transport regulation.

A causative link between axonal transport disruptions and competitive weakness has to be proven. *In vivo* imaging of axonal transport would probably be necessary to correlate the time course of transport reductions and the elimination of inputs.

Summary

My thesis set out to test the hypothesis of disturbed axonal transport in two models of 'die-back' axon loss: The first part aimed at clarifying the relationship between organelle transport deficits and degenerative changes in a mouse model of motor neuron disease (Part 1). The second part contains the exploration of transport changes in dismantling branches during development (Part 2). I used techniques which allowed measuring axonal transport in living axons and axon branches within their natural habitat (Misgeld, Kerschensteiner et al. 2007). The techniques used in my thesis were detailed in Nature Protocols 2008 (Kerschensteiner, Reuter et al., 2008).

Part 1: This part of my thesis represents the characterization of mitochondrial transport throughout the disease course of the most widely used ALS model, the SOD^{G93A} mouse. My results showed a profound reduction in mitochondrial flux months before symptoms or neuromuscular denervation appeared. The transport deficit affected both anterograde and retrograde direction. Anterograde transport was significantly reduced at P20, whereas statistically significant differences in retrograde transport could first be detected around P60. The average velocity of moving mitochondria was reduced. This slowing originated from a higher frequency of pauses, an increase in the frequency of intermediate velocities and a reduction in maximum velocity. Analysis of transport on the level of individual axons revealed heterogeneity within SOD^{G93A} axons, with some axons apparently not affected by the transport deficit. Mitochondrial morphology in SOD^{G93A} intercostal motor axons was altered. They were shorter and rounder than in control animals. These morphologic changes could not be detected in axons innervating extra-ocular muscles, which are also otherwise spared in ALS.

In contrast to my results in SOD^{G93A} mice, follow-up studies by my colleague P. Marinkovic on the SOD^{G85R} and SOD^{WT} mouse lines revealed that degeneration could occur in the absence of a transport deficit and a transport deficit did not necessarily lead to neurodegeneration. His results argued against a primary causative role of axonal transport in motor neuron diseases. The results of our combined study were published in PNAS in 2012 (Marinkovic, Reuter et al. 2012).

Part 2: The second part of my thesis was to measure mitochondrial transport during the transition from multiple- to single-innervation at the neuromuscular junction. My results showed profound reductions of both anterograde and retrograde mitochondrial transport within axon branches that were currently undergoing elimination. A reduction in transport was

already apparent in morphologically atrophic axon branches that were likely to undergo elimination but had not yet lost contact to the muscle fiber. In doubly innervated neuromuscular junctions I found a significant correlation of mitochondrial transport with axon diameter. Axon branches that had successfully competed against other inputs and hence innervated a singly innervated muscle fiber, as well as putative 'winner' branches in doubly innervated neuromuscular junctions, had increased transport, compared to branches that were still in competition with open outcome. As reductions in axonal transport did occur in atrophic and dismantling branches, it represents a plausible mechanism to mediate competition between converging inputs. Further characterization of the transport-to-fate correlations that I discovered for motor axon branches during synapse elimination, as well as experimental interventions to explore whether the discovered correlations result from causative relationships are ongoing in our lab. Publication of these results is projected for 2013.

In conclusion, my data revealed the presence of axonal transport reductions in a mouse model of motor neuron disease and in dismantling axon branches during development. Whether such changes could play a causative, respectively regulatory role in the different forms of axon loss, remains elusive and is the topic of ongoing studies in our and other labs. A disruption in axonal transport remains a promising link between physiologically occurring axon loss and pathological axon degeneration.

Appendix

Reagents:

Isofluran as lethal anaesthetic for adult mice (anaesthesia was performed under a chemical fume hood)

Ketamine-xylazine (1.5% ketamine, 0.1% xylazine; protocol below) injected i.p. as lethal anaesthetics for pubs

1x Ringer's solution (protocol below)

Carbogen (95% O_2/ 5% CO_2)

70% (volume/volume) ethanol in spray bottle

0.01M Phosphate-buffered saline (1x PBS)

1x PBS/0.1% (weight/volume) NaN_3

4% Paraformaldehyde (PFA; weight/volume) in 1x PBS (protocol below)

Alexa594-conjugated α-bungarotoxin (BTX) (Invitrogen)

Antifading medium for fluorescence microscopy (Vectashield, Vector Laboratories)

Immersion oil for confocal microscopy

Equipment:

Chemical fume hood

Glass container for Isoflurane anaesthesia

1ml syringe with fine hypodermic needle for i.p. injection of ketamine-xylazine

Large medical scissors

Small-angled spring scissors

2x Anatomical forceps, size 1 and 5

2x 10-cm Tissue culture dishes with oxygenated medium

15-cm Tissue culture dish filled with ice and covered by a metal plate

3.5-cm Tissue culture dish filled with Sylgard polymer (Dow Corning)

10x Minuten pins (0.2-mm diameter, shortened to <4 mm) to fix explanted tissue in the dish

Tubing to oxygenate explants during the dissection procedure

Dissection microscope with cold-light illumination (Olympus SZ51 equipped with Schott KL 1500 LCD)

Upright fluorescence microscope (BX51WI, Olympus) equipped with the following long-working distance objectives: 4x/ N.A. 0.13 air objective; 20x/ N.A. 0.5 water-immersion dipping-cone objective; 100x/ N.A. 1.0 water immersion dipping-cone objective, filters for

fluorescent proteins: ET F46-001 for CFP, ET F46-003 for YFP, ET F46-008 for TxRED; AHF Analysentechnik, Germany)

Gravity-driven superfusion system with in-line heater (Warner Instruments)

Vacuum system with suction tube

Heating ring for 3.5-cm dishes (Warner Instruments)

Two-channel temperature control system (one output for the in-line heater and one output for the heating ring; input for a temperature probe (Warner Instruments))

Arc lamp

Neutral-density and infrared-filters in light path (U25ND25 and U25ND6; Olympus)

Fast shutter and filter wheel (Sutter Instrument Company)

Light source with light-guide for oblique illumination (Linos)

Cooled charge-coupled device (CCD) camera (SensicamQE (Cooke)

Computer and control software (TillVision)

x–y alignment software (ImageJ with 'stackreg' plugin)

Graphics software (Photoshop, Adobe)

Upright confocal microscope (FV1000, Olympus) equipped the following objectives: 60x/ N.A. 1.42 and 20x/ N.A. 0.85 oil objectives, and 10x/ N.A. 0.40 and 4x/ N.A. 0.13 air objectives

Dissection tools for fixed tissue:

Razor blade

Anatomical tweezers

1-ml syringe with hypodermic needle for fine dissection

Small-angled spring scissors with pointed tips

2x hypodermic needles (G23) to pin down tissue

10-cm tissue culture dish filled with Sylgard polymer

Slides and coverslips (no. 1.5)

Protocols:

Mouse breeding

Thy1-MitoCFP heterozygous or homozygous female mice were crossed with *SOD*^{G93A} heterozygous males. Double-transgenic *thy1-MitoCFP, SOD*^{G93A} and *thy1-MitoCFP* controls were identified by PCR from tail biopsies.

To score for denervation *thy1-YFP*^{16} homozygous female mice were crossed with *SOD*^{G93A} heterozygous males. Double-transgenic *thy1-YFP*^{16}, *SOD*^{G93A} and *thy1-YFP*^{16} controls were identified by PCR from tail biopsies.

Thy1-MitoCFP^{K} homozygous females or males were crossed with *thy1-YFP*^{16} homozygous males or females. All littermates were double-heterozygous *thy1-MitoCFP*^{K}, *thy1-YFP*^{16} and could be used for imaging studies.

10x PBS (100mM = 0.1M)

- 2.6g $NaH_2PO_4*H_2O$
- 14.4g $Na_2HPO_4*2H_2O$
- 87.5g NaCl
- 900ml reverse-osmosis (Membrapur) water

The pH was adjusted to 7.2 – 7.4 at room temperature with

- 1N NaOH
- 1N HCl

The solution was filtrated through a 0.22µm filter and stored at room temperature. For long term storage it was transferred to 4°C. To obtain 1x PBS (10mM = 0.01M) the solution was diluted 1:10 in reverse-osmosis H_2O.

Blocking solution for antibody staining

- 50ml goat serum
- 10g bovine serum albumin (BSA)
- 2ml Triton
- 1ml 20% sodium azide (NaN_3)

The reagents were filled up to 1l with 1x PBS and warmed in water bath until everything was dissolved. The solution was filtrated through a 0.22µm filter and stored at -20°C.

Ketamine-xylazine

- 300mg ketamine (Sigma)
- 20mg xylazine (Sigma)

The reagents were filled up to 20ml with H_2O, the solution was filtered through a 0.22µm filter.

Ringer's solution (10x)

- 21.84g $NaHCO_3$
- 1.72g $NaH_2PO_4*H_2O$
- 1.86g KCl (25mM)
- 73.05g NaCl

The reagents were filled up to 1l with H_2O. The solution was filtrated through a 0.22µm filter.

Ringer's solution (1x)

- 2ml 1M $CaCl_2$
- 900ml H_2O
- 1ml 1M $MgCl_2$
- 100ml 10x Ringer's solution
- 3.6g Glucose

1x Ringer's solution was bubbled with 95% O_2/5% CO_2 for at least 30min before use, to generate a pH of 7.3.

BTX staining

- Triangularis sterni samples were washed in 1x PBS and were transferred to 25 well plates
- Incubated in blocking solution for one hour at room temperature on an orbital shaker
- Stained with Alexa594-BTX, 2.5µg/ml for 1h at 4°C (on orbital shaker)
- Washed in 1x PBS for at least 1h
- Mounted on microscope slides with Vectashield antifading medium

Literature

Ahmadi, M., J. X. Liu, T. Brannstrom, P. M. Andersen, P. Stal and F. Pedrosa-Domellof (2010). "Human extraocular muscles in ALS." Invest Ophthalmol Vis Sci **51**(7): 3494-3501.

Alexander, G. M., K. L. Erwin, N. Byers, J. S. Deitch, B. J. Augelli, E. P. Blankenhorn and T. D. Heiman-Patterson (2004). "Effect of transgene copy number on survival in the G93A SOD1 transgenic mouse model of ALS." Brain Res Mol Brain Res **130**(1-2): 7-15.

Azzouz, M., A. Hottinger, J. C. Paterna, A. D. Zurn, P. Aebischer and H. Bueler (2000). "Increased motoneuron survival and improved neuromuscular function in transgenic ALS mice after intraspinal injection of an adeno-associated virus encoding Bcl-2." Hum Mol Genet **9**(5): 803-811.

Bacman, S. R., W. G. Bradley and C. T. Moraes (2006). "Mitochondrial involvement in amyotrophic lateral sclerosis: trigger or target?" Mol Neurobiol **33**(2): 113-131.

Balice-Gordon, R. J., C. K. Chua, C. C. Nelson and J. W. Lichtman (1993). "Gradual loss of synaptic cartels precedes axon withdrawal at developing neuromuscular junctions." Neuron **11**(5): 801-815.

Balice-Gordon, R. J. and J. W. Lichtman (1994). "Long-term synapse loss induced by focal blockade of postsynaptic receptors." Nature **372**(6506): 519-524.

Barber, M. J. and J. W. Lichtman (1999). "Activity-driven synapse elimination leads paradoxically to domination by inactive neurons." J Neurosci **19**(22): 9975-9985.

Beers, D. R., J. S. Henkel, Q. Xiao, W. Zhao, J. Wang, A. A. Yen, L. Siklos, S. R. McKercher and S. H. Appel (2006). "Wild-type microglia extend survival in PU.1 knockout mice with familial amyotrophic lateral sclerosis." Proc Natl Acad Sci U S A **103**(43): 16021-16026.

Bensimon, G., L. Lacomblez and V. Meininger (1994). "A controlled trial of riluzole in amyotrophic lateral sclerosis. ALS/Riluzole Study Group." N Engl J Med **330**(9): 585-591.

Bernstein, M. and J. W. Lichtman (1999). "Axonal atrophy: the retraction reaction." Curr Opin Neurobiol **9**(3): 364-370.

Bilsland, L. G., E. Sahai, G. Kelly, M. Golding, L. Greensmith and G. Schiavo (2010). "Deficits in axonal transport precede ALS symptoms in vivo." Proc Natl Acad Sci U S A **107**(47): 20523-20528.

Bishop, D. L., T. Misgeld, M. K. Walsh, W. B. Gan and J. W. Lichtman (2004). "Axon branch removal at developing synapses by axosome shedding." Neuron **44**(4): 651-661.

Boillee, S., C. Vande Velde and D. W. Cleveland (2006). "ALS: a disease of motor neurons and their nonneuronal neighbors." Neuron **52**(1): 39-59.

Bosco, D. A., G. Morfini, N. M. Karabacak, Y. Song, F. Gros-Louis, P. Pasinelli, H. Goolsby, B. A. Fontaine, N. Lemay, D. McKenna-Yasek, M. P. Frosch, J. N. Agar, J. P. Julien, S. T. Brady and R. H. Brown, Jr. (2010). "Wild-type and mutant SOD1 share an aberrant conformation and a common pathogenic pathway in ALS." Nat Neurosci **13**(11): 1396-1403.

Bowling, A. C., J. B. Schulz, R. H. Brown, Jr. and M. F. Beal (1993). "Superoxide dismutase activity, oxidative damage, and mitochondrial energy metabolism in familial and sporadic amyotrophic lateral sclerosis." J Neurochem **61**(6): 2322-2325.

Brady, S. T., K. K. Pfister and G. S. Bloom (1990). "A monoclonal antibody against kinesin inhibits both anterograde and retrograde fast axonal transport in squid axoplasm." Proc Natl Acad Sci U S A **87**(3): 1061-1065.

Breuer, A. C., M. P. Lynn, M. B. Atkinson, S. M. Chou, A. J. Wilbourn, K. E. Marks, J. E. Culver and E. J. Fleegler (1987). "Fast axonal transport in amyotrophic lateral sclerosis: an intra-axonal organelle traffic analysis." Neurology **37**(5): 738-748.

Brill, M. S., J. W. Lichtman, W. Thompson, Y. Zuo and T. Misgeld (2011). "Spatial constraints dictate glial territories at murine neuromuscular junctions." J Cell Biol **195**(2): 293-305.

Bruijn, L. I., M. W. Becher, M. K. Lee, K. L. Anderson, N. A. Jenkins, N. G. Copeland, S. S. Sisodia, J. D. Rothstein, D. R. Borchelt, D. L. Price and D. W. Cleveland (1997). "ALS-linked SOD1 mutant

G85R mediates damage to astrocytes and promotes rapidly progressive disease with SOD1-containing inclusions." Neuron **18**(2): 327-338.

Buffelli, M., R. W. Burgess, G. Feng, C. G. Lobe, J. W. Lichtman and J. R. Sanes (2003). "Genetic evidence that relative synaptic efficacy biases the outcome of synaptic competition." Nature **424**(6947): 430-434.

Cai, Q. and Z. H. Sheng (2009). "Mitochondrial transport and docking in axons." Exp Neurol **218**(2): 257-267.

Chada, S. R. and P. J. Hollenbeck (2003). "Mitochondrial movement and positioning in axons: the role of growth factor signaling." J Exp Biol **206**(Pt 12): 1985-1992.

Chen, S., G. C. Owens, K. L. Crossin and D. B. Edelman (2007). "Serotonin stimulates mitochondrial transport in hippocampal neurons." Mol Cell Neurosci **36**(4): 472-483.

Chen, S., G. C. Owens and D. B. Edelman (2008). "Dopamine inhibits mitochondrial motility in hippocampal neurons." PLoS One **3**(7): e2804.

Chevalier-Larsen, E. and E. L. Holzbaur (2006). "Axonal transport and neurodegenerative disease." Biochim Biophys Acta **1762**(11-12): 1094-1108.

Coleman, M. P., L. Conforti, E. A. Buckmaster, A. Tarlton, R. M. Ewing, M. C. Brown, M. F. Lyon and V. H. Perry (1998). "An 85-kb tandem triplication in the slow Wallerian degeneration (Wlds) mouse." Proc Natl Acad Sci U S A **95**(17): 9985-9990.

Coleman, M. P. and M. R. Freeman (2010). "Wallerian degeneration, wld(s), and nmnat." Annu Rev Neurosci **33**: 245-267.

Coleman, M. P. and V. H. Perry (2002). "Axon pathology in neurological disease: a neglected therapeutic target." Trends Neurosci **25**(10): 532-537.

Collard, J. F., F. Cote and J. P. Julien (1995). "Defective axonal transport in a transgenic mouse model of amyotrophic lateral sclerosis." Nature **375**(6526): 61-64.

Cote, F., J. F. Collard and J. P. Julien (1993). "Progressive neuronopathy in transgenic mice expressing the human neurofilament heavy gene: a mouse model of amyotrophic lateral sclerosis." Cell **73**(1): 35-46.

Couillard-Despres, S., Q. Zhu, P. C. Wong, D. L. Price, D. W. Cleveland and J. P. Julien (1998). "Protective effect of neurofilament heavy gene overexpression in motor neuron disease induced by mutant superoxide dismutase." Proc Natl Acad Sci U S A **95**(16): 9626-9630.

Cowan, C. M., T. Bossing, A. Page, D. Shepherd and A. Mudher (2010). "Soluble hyper-phosphorylated tau causes microtubule breakdown and functionally compromises normal tau in vivo." Acta Neuropathol **120**(5): 593-604.

Cowan, W. M., J. W. Fawcett, D. D. O'Leary and B. B. Stanfield (1984). "Regressive events in neurogenesis." Science **225**(4668): 1258-1265.

De Vos, K. J., A. L. Chapman, M. E. Tennant, C. Manser, E. L. Tudor, K. F. Lau, J. Brownlees, S. Ackerley, P. J. Shaw, D. M. McLoughlin, C. E. Shaw, P. N. Leigh, C. C. Miller and A. J. Grierson (2007). "Familial amyotrophic lateral sclerosis-linked SOD1 mutants perturb fast axonal transport to reduce axonal mitochondria content." Hum Mol Genet **16**(22): 2720-2728.

De Vos, K. J., A. J. Grierson, S. Ackerley and C. C. Miller (2008). "Role of axonal transport in neurodegenerative diseases." Annu Rev Neurosci **31**: 151-173.

Di Giorgio, F. P., M. A. Carrasco, M. C. Siao, T. Maniatis and K. Eggan (2007). "Non-cell autonomous effect of glia on motor neurons in an embryonic stem cell-based ALS model." Nat Neurosci **10**(5): 608-614.

Dimos, J. T., K. T. Rodolfa, K. K. Niakan, L. M. Weisenthal, H. Mitsumoto, W. Chung, G. F. Croft, G. Saphier, R. Leibel, R. Goland, H. Wichterle, C. E. Henderson and K. Eggan (2008). "Induced pluripotent stem cells generated from patients with ALS can be differentiated into motor neurons." Science **321**(5893): 1218-1221.

Dixit, R., J. L. Ross, Y. E. Goldman and E. L. Holzbaur (2008). "Differential regulation of dynein and kinesin motor proteins by tau." Science **319**(5866): 1086-1089.

Donaghy, C., M. J. Thurtell, E. P. Pioro, J. M. Gibson and R. J. Leigh (2011). "Eye movements in amyotrophic lateral sclerosis and its mimics: a review with illustrative cases." J Neurol Neurosurg Psychiatry **82**(1): 110-116.

Duncan, J. E. and L. S. Goldstein (2006). "The genetics of axonal transport and axonal transport disorders." PLoS Genet **2**(9): e124.

Durham, H. D., J. Roy, L. Dong and D. A. Figlewicz (1997). "Aggregation of mutant Cu/Zn superoxide dismutase proteins in a culture model of ALS." J Neuropathol Exp Neurol **56**(5): 523-530.

Fanara, P., J. Banerjee, R. V. Hueck, M. R. Harper, M. Awada, H. Turner, K. H. Husted, R. Brandt and M. K. Hellerstein (2007). "Stabilization of hyperdynamic microtubules is neuroprotective in amyotrophic lateral sclerosis." J Biol Chem **282**(32): 23465-23472.

Fanara, P., P. Y. Wong, K. H. Husted, S. Liu, V. M. Liu, L. A. Kohlstaedt, T. Riiff, J. C. Protasio, D. Boban, S. Killion, M. Killian, L. Epling, E. Sinclair, J. Peterson, R. W. Price, D. E. Cabin, R. L. Nussbaum, J. Bruhmann, R. Brandt, C. W. Christine, M. J. Aminoff and M. K. Hellerstein (2012). "Cerebrospinal fluid-based kinetic biomarkers of axonal transport in monitoring neurodegeneration." J Clin Invest **122**(9): 3159-3169.

Feng, G., R. H. Mellor, M. Bernstein, C. Keller-Peck, Q. T. Nguyen, M. Wallace, J. M. Nerbonne, J. W. Lichtman and J. R. Sanes (2000). "Imaging neuronal subsets in transgenic mice expressing multiple spectral variants of GFP." Neuron **28**(1): 41-51.

Ferri, A., J. R. Sanes, M. P. Coleman, J. M. Cunningham and A. C. Kato (2003). "Inhibiting axon degeneration and synapse loss attenuates apoptosis and disease progression in a mouse model of motoneuron disease." Curr Biol **13**(8): 669-673.

Fischer, L. R., D. G. Culver, P. Tennant, A. A. Davis, M. Wang, A. Castellano-Sanchez, J. Khan, M. A. Polak and J. D. Glass (2004). "Amyotrophic lateral sclerosis is a distal axonopathy: evidence in mice and man." Exp Neurol **185**(2): 232-240.

Frey, D., C. Schneider, L. Xu, J. Borg, W. Spooren and P. Caroni (2000). "Early and selective loss of neuromuscular synapse subtypes with low sprouting competence in motoneuron diseases." J Neurosci **20**(7): 2534-2542.

Gazzola, M., C. J. Burckhardt, B. Bayati, M. Engelke, U. F. Greber and P. Koumoutsakos (2009). "A stochastic model for microtubule motors describes the in vivo cytoplasmic transport of human adenovirus." PLoS Comput Biol **5**(12): e1000623.

Goldstein, A. Y., X. Wang and T. L. Schwarz (2008). "Axonal transport and the delivery of pre-synaptic components." Curr Opin Neurobiol **18**(5): 495-503.

Gong, Y. H., A. S. Parsadanian, A. Andreeva, W. D. Snider and J. L. Elliott (2000). "Restricted expression of G86R Cu/Zn superoxide dismutase in astrocytes results in astrocytosis but does not cause motoneuron degeneration." J Neurosci **20**(2): 660-665.

Guiheneuc, P., J. Ginet, J. Y. Groleau and J. Rojouan (1980). "Early phase of vincristine neuropathy in man. Electrophysiological evidence for a dying-back phenomenon, with transitory enhancement of spinal transmission of the monosynaptic reflex." J Neurol Sci **45**(2-3): 355-366.

Gurney, M. E., H. Pu, A. Y. Chiu, M. C. Dal Canto, C. Y. Polchow, D. D. Alexander, J. Caliendo, A. Hentati, Y. W. Kwon, H. X. Deng and et al. (1994). "Motor neuron degeneration in mice that express a human Cu,Zn superoxide dismutase mutation." Science **264**(5166): 1772-1775.

Haass-Mannle, H. and H. W. Zimmermann (1997). "Selective photoaffinity labelling of one mitochondrial protein in living cells of Saccharomyces cerevisiae with the fluorescent probe APMC. Identification of the target protein as subunit I of cytochrome c oxidase." J Photochem Photobiol B **41**(1-2): 90-102.

Hafezparast, M., R. Klocke, C. Ruhrberg, A. Marquardt, A. Ahmad-Annuar, S. Bowen, G. Lalli, A. S. Witherden, H. Hummerich, S. Nicholson, P. J. Morgan, R. Oozageer, J. V. Priestley, S. Averill, V. R. King, S. Ball, J. Peters, T. Toda, A. Yamamoto, Y. Hiraoka, M. Augustin, D. Korthaus, S. Wattler, P. Wabnitz, C. Dickneite, S. Lampel, F. Boehme, G. Peraus, A. Popp, M. Rudelius, J. Schlegel, H. Fuchs, M. Hrabe de Angelis, G. Schiavo, D. T. Shima, A. P. Russ, G. Stumm, J. E.

Martin and E. M. Fisher (2003). "Mutations in dynein link motor neuron degeneration to defects in retrograde transport." Science **300**(5620): 808-812.
Heiman-Patterson, T. D., J. S. Deitch, E. P. Blankenhorn, K. L. Erwin, M. J. Perreault, B. K. Alexander, N. Byers, I. Toman and G. M. Alexander (2005). "Background and gender effects on survival in the TgN(SOD1-G93A)1Gur mouse model of ALS." J Neurol Sci **236**(1-2): 1-7.
Higgins, C. M., C. Jung and Z. Xu (2003). "ALS-associated mutant SOD1G93A causes mitochondrial vacuolation by expansion of the intermembrane space and by involvement of SOD1 aggregation and peroxisomes." BMC Neurosci **4**: 16.
Hirano, A., H. Donnenfeld, S. Sasaki and I. Nakano (1984). "Fine structural observations of neurofilamentous changes in amyotrophic lateral sclerosis." J Neuropathol Exp Neurol **43**(5): 461-470.
Hirano, A., I. Nakano, L. T. Kurland, D. W. Mulder, P. W. Holley and G. Saccomanno (1984). "Fine structural study of neurofibrillary changes in a family with amyotrophic lateral sclerosis." J Neuropathol Exp Neurol **43**(5): 471-480.
Hirokawa, N. (1982). "Cross-linker system between neurofilaments, microtubules, and membranous organelles in frog axons revealed by the quick-freeze, deep-etching method." J Cell Biol **94**(1): 129-142.
Hollenbeck, P. J. (1996). "The pattern and mechanism of mitochondrial transport in axons." Front Biosci **1**: d91-102.
Hollenbeck, P. J. and W. M. Saxton (2005). "The axonal transport of mitochondria." J Cell Sci **118**(Pt 23): 5411-5419.
Igoudjil, A., J. Magrane, L. R. Fischer, H. J. Kim, I. Hervias, M. Dumont, C. Cortez, J. D. Glass, A. A. Starkov and G. Manfredi (2011). "In vivo pathogenic role of mutant SOD1 localized in the mitochondrial intermembrane space." J Neurosci **31**(44): 15826-15837.
Ince, P., N. Stout, P. Shaw, J. Slade, W. Hunziker, C. W. Heizmann and K. G. Baimbridge (1993). "Parvalbumin and calbindin D-28k in the human motor system and in motor neuron disease." Neuropathol Appl Neurobiol **19**(4): 291-299.
Julien, J. P. (2007). "ALS: astrocytes move in as deadly neighbors." Nat Neurosci **10**(5): 535-537.
Julien, J. P., F. Cote and J. F. Collard (1995). "Mice overexpressing the human neurofilament heavy gene as a model of ALS." Neurobiol Aging **16**(3): 487-490; discussion 490-482.
Julien, J. P. and W. E. Mushynski (1998). "Neurofilaments in health and disease." Prog Nucleic Acid Res Mol Biol **61**: 1-23.
Jung, C., C. M. Higgins and Z. Xu (2002). "Mitochondrial electron transport chain complex dysfunction in a transgenic mouse model for amyotrophic lateral sclerosis." J Neurochem **83**(3): 535-545.
Kang, J. S., J. H. Tian, P. Y. Pan, P. Zald, C. Li, C. Deng and Z. H. Sheng (2008). "Docking of axonal mitochondria by syntaphilin controls their mobility and affects short-term facilitation." Cell **132**(1): 137-148.
Kasthuri, N. and J. W. Lichtman (2003). "The role of neuronal identity in synaptic competition." Nature **424**(6947): 426-430.
Kato, S., Y. Saeki, M. Aok, M. Nagai, A. Ishigaki, Y. Itoyama, M. Kato, K. Asayama, A. Awaya, A. Hirano, E. Ohama (2004). "Histological evidence of redox system breakdown caused by superoxide dismutase 1 (SOD1) aggregation is common to SOD1-mutated motor neurons in humans and animal models." Acta Neuropathol **107**(2):149-58.
Keller-Peck, C. R., M. K. Walsh, W. B. Gan, G. Feng, J. R. Sanes and J. W. Lichtman (2001). "Asynchronous synapse elimination in neonatal motor units: studies using GFP transgenic mice." Neuron **31**(3): 381-394.
Kerschensteiner, M., M. S. Reuter, J. W. Lichtman and T. Misgeld (2008). "Ex vivo imaging of motor axon dynamics in murine triangularis sterni explants." Nat Protoc **3**(10): 1645-1653.
Kieran, D., M. Hafezparast, S. Bohnert, J. R. Dick, J. Martin, G. Schiavo, E. M. Fisher and L. Greensmith (2005). "A mutation in dynein rescues axonal transport defects and extends the life span of ALS mice." J Cell Biol **169**(4): 561-567.

Kirkpatrick, L. L. and S. T. Brady (1994). "Modulation of the axonal microtubule cytoskeleton by myelinating Schwann cells." J Neurosci **14**(12): 7440-7450.

Kiryu-Seo, S., N. Ohno, G. J. Kidd, H. Komuro and B. D. Trapp (2010). "Demyelination increases axonal stationary mitochondrial size and the speed of axonal mitochondrial transport." J Neurosci **30**(19): 6658-6666.

LaMonte, B. H., K. E. Wallace, B. A. Holloway, S. S. Shelly, J. Ascano, M. Tokito, T. Van Winkle, D. S. Howland and E. L. Holzbaur (2002). "Disruption of dynein/dynactin inhibits axonal transport in motor neurons causing late-onset progressive degeneration." Neuron **34**(5): 715-727.

Letourneau, P. C. (2009). "Actin in axons: stable scaffolds and dynamic filaments." Results Probl Cell Differ **48**: 65-90.

Lichtman, J. W. and H. Colman (2000). "Synapse elimination and indelible memory." Neuron **25**(2): 269-278.

Ligon, L. A., B. H. LaMonte, K. E. Wallace, N. Weber, R. G. Kalb and E. L. Holzbaur (2005). "Mutant superoxide dismutase disrupts cytoplasmic dynein in motor neurons." Neuroreport **16**(6): 533-536.

Lino, M. M., C. Schneider and P. Caroni (2002). "Accumulation of SOD1 mutants in postnatal motoneurons does not cause motoneuron pathology or motoneuron disease." J Neurosci **22**(12): 4825-4832.

Liu, D., J. Wen, J. Liu and L. Li (1999). "The roles of free radicals in amyotrophic lateral sclerosis: reactive oxygen species and elevated oxidation of protein, DNA, and membrane phospholipids." FASEB J **13**(15): 2318-2328.

Liu, Z., Y. Chen, D. Wang, S. Wang and Y. Q. Zhang (2010). "Distinct presynaptic and postsynaptic dismantling processes of Drosophila neuromuscular junctions during metamorphosis." J Neurosci **30**(35): 11624-11634.

Luo, L. and D. D. O'Leary (2005). "Axon retraction and degeneration in development and disease." Annu Rev Neurosci **28**: 127-156.

Magrane, J., I. Hervias, M. S. Henning, M. Damiano, H. Kawamata and G. Manfredi (2009). "Mutant SOD1 in neuronal mitochondria causes toxicity and mitochondrial dynamics abnormalities." Hum Mol Genet **18**(23): 4552-4564.

Magrane, J. and G. Manfredi (2009). "Mitochondrial function, morphology, and axonal transport in amyotrophic lateral sclerosis." Antioxid Redox Signal **11**(7): 1615-1626.

Magrane, J., M. A. Sahawneh, S. Przedborski, A. G. Estevez and G. Manfredi (2012). "Mitochondrial dynamics and bioenergetic dysfunction is associated with synaptic alterations in mutant SOD1 motor neurons." J Neurosci **32**(1): 229-242.

Marinkovic, P., M. S. Reuter, M. S. Brill, L. Godinho, M. Kerschensteiner and T. Misgeld (2012). "Axonal transport deficits and degeneration can evolve independently in mouse models of amyotrophic lateral sclerosis." Proc Natl Acad Sci U S A **109**(11): 4296-4301.

Mattiazzi, M., M. D'Aurelio, C. D. Gajewski, K. Martushova, M. Kiaei, M. F. Beal and G. Manfredi (2002). "Mutated human SOD1 causes dysfunction of oxidative phosphorylation in mitochondria of transgenic mice." J Biol Chem **277**(33): 29626-29633.

McQuarrie, I. G., S. T. Brady and R. J. Lasek (1989). "Retardation in the slow axonal transport of cytoskeletal elements during maturation and aging." Neurobiol Aging **10**(4): 359-365.

Miki, H., M. Setou, K. Kaneshiro and N. Hirokawa (2001). "All kinesin superfamily protein, KIF, genes in mouse and human." Proc Natl Acad Sci U S A **98**(13): 7004-7011.

Miller, K. E. and M. P. Sheetz (2004). "Axonal mitochondrial transport and potential are correlated." J Cell Sci **117**(Pt 13): 2791-2804.

Minoshima, S. and D. Cross (2008). "In vivo imaging of axonal transport using MRI: aging and Alzheimer's disease." Eur J Nucl Med Mol Imaging **35 Suppl 1**: S89-92.

Misgeld, T. (2005). "Death of an axon: studying axon loss in development and disease." Histochem Cell Biol **124**(3-4): 189-196.

Misgeld, T., M. Kerschensteiner, F. M. Bareyre, R. W. Burgess and J. W. Lichtman (2007). "Imaging axonal transport of mitochondria in vivo." Nat Methods **4**(7): 559-561.

Morris, R. L. and P. J. Hollenbeck (1995). "Axonal transport of mitochondria along microtubules and F-actin in living vertebrate neurons." J Cell Biol **131**(5): 1315-1326.

Murrey, H. E. and L. C. Hsieh-Wilson (2008). "The chemical neurobiology of carbohydrates." Chem Rev **108**(5): 1708-1731.

Nagai, M., D. B. Re, T. Nagata, A. Chalazonitis, T. M. Jessell, H. Wichterle and S. Przedborski (2007). "Astrocytes expressing ALS-linked mutated SOD1 release factors selectively toxic to motor neurons." Nat Neurosci **10**(5): 615-622.

Ohno, N., G. J. Kidd, D. Mahad, S. Kiryu-Seo, A. Avishai, H. Komuro and B. D. Trapp (2011). "Myelination and axonal electrical activity modulate the distribution and motility of mitochondria at CNS nodes of Ranvier." J Neurosci **31**(20): 7249-7258.

Oppenheim, R. W. (1991). "Cell death during development of the nervous system." Annu Rev Neurosci **14**: 453-501.

Parson, S. H., C. L. Mackintosh and R. R. Ribchester (1997). "Elimination of motor nerve terminals in neonatal mice expressing a gene for slow wallerian degeneration (C57Bl/Wlds)." Eur J Neurosci **9**(8): 1586-1592.

Perlson, E., G. B. Jeong, J. L. Ross, R. Dixit, K. E. Wallace, R. G. Kalb and E. L. Holzbaur (2009). "A switch in retrograde signaling from survival to stress in rapid-onset neurodegeneration." J Neurosci **29**(31): 9903-9917.

Personius, K. E. and R. J. Balice-Gordon (2001). "Loss of correlated motor neuron activity during synaptic competition at developing neuromuscular synapses." Neuron **31**(3): 395-408.

Pesiridis, G. S., K. Tripathy, S. Tanik, J. Q. Trojanowski and V. M. Lee (2011). "A "two-hit" hypothesis for inclusion formation by carboxyl-terminal fragments of TDP-43 protein linked to RNA depletion and impaired microtubule-dependent transport." J Biol Chem **286**(21): 18845-18855.

Pugdahl, K., A. Fuglsang-Frederiksen, M. de Carvalho, B. Johnsen, P. R. Fawcett, A. Labarre-Vila, R. Liguori, W. A. Nix and I. S. Schofield (2007). "Generalised sensory system abnormalities in amyotrophic lateral sclerosis: a European multicentre study." J Neurol Neurosurg Psychiatry **78**(7): 746-749.

Puls, I., C. Jonnakuty, B. H. LaMonte, E. L. Holzbaur, M. Tokito, E. Mann, M. K. Floeter, K. Bidus, D. Drayna, S. J. Oh, R. H. Brown, Jr., C. L. Ludlow and K. H. Fischbeck (2003). "Mutant dynactin in motor neuron disease." Nat Genet **33**(4): 455-456.

Pun, S., A. F. Santos, S. Saxena, L. Xu and P. Caroni (2006). "Selective vulnerability and pruning of phasic motoneuron axons in motoneuron disease alleviated by CNTF." Nat Neurosci **9**(3): 408-419.

Reaume, A. G., J. L. Elliott, E. K. Hoffman, N. W. Kowall, R. J. Ferrante, D. F. Siwek, H. M. Wilcox, D. G. Flood, M. F. Beal, R. H. Brown, Jr., R. W. Scott and W. D. Snider (1996). "Motor neurons in Cu/Zn superoxide dismutase-deficient mice develop normally but exhibit enhanced cell death after axonal injury." Nat Genet **13**(1): 43-47.

Riley, D. A. (1977). "Spontaneous elimination of nerve terminals from the endplates of developing skeletal myofibers." Brain Res **134**(2): 279-285.

Riley, D. A. (1981). "Ultrastructural evidence for axon retraction during the spontaneous elimination of polyneuronal innervation of the rat soleus muscle." J Neurocytol **10**(3): 425-440.

Rosen, D. R., T. Siddique, D. Patterson, D. A. Figlewicz, P. Sapp, A. Hentati, D. Donaldson, J. Goto, J. P. O'Regan, H. X. Deng and et al. (1993). "Mutations in Cu/Zn superoxide dismutase gene are associated with familial amyotrophic lateral sclerosis." Nature **362**(6415): 59-62.

Rothstein, J. D. (2009). "Current hypotheses for the underlying biology of amyotrophic lateral sclerosis." Ann Neurol **65 Suppl 1**: S3-9.

Rothstein, J. D., M. Dykes-Hoberg, C. A. Pardo, L. A. Bristol, L. Jin, R. W. Kuncl, Y. Kanai, M. A. Hediger, Y. Wang, J. P. Schielke and D. F. Welty (1996). "Knockout of glutamate transporters reveals a major role for astroglial transport in excitotoxicity and clearance of glutamate." Neuron **16**(3): 675-686.

Sanes, J. R. and J. W. Lichtman (1999). "Development of the vertebrate neuromuscular junction." Annu Rev Neurosci **22**: 389-442.

Sasaki, S. and M. Iwata (1996). "Impairment of fast axonal transport in the proximal axons of anterior horn neurons in amyotrophic lateral sclerosis." Neurology **47**(2): 535-540.

Sasaki, S. and M. Iwata (2007). "Mitochondrial alterations in the spinal cord of patients with sporadic amyotrophic lateral sclerosis." J Neuropathol Exp Neurol **66**(1): 10-16.

Schaefer, A. M., J. R. Sanes and J. W. Lichtman (2005). "A compensatory subpopulation of motor neurons in a mouse model of amyotrophic lateral sclerosis." J Comp Neurol **490**(3): 209-219.

Shan, X., P. M. Chiang, D. L. Price and P. C. Wong (2010). "Altered distributions of Gemini of coiled bodies and mitochondria in motor neurons of TDP-43 transgenic mice." Proc Natl Acad Sci U S A **107**(37): 16325-16330.

Shibata, N., R. Nagai, K. Uchida, S. Horiuchi, S. Yamada, A. Hirano, M. Kawaguchi, T. Yamamoto, S. Sasaki and M. Kobayashi (2001). "Morphological evidence for lipid peroxidation and protein glycoxidation in spinal cords from sporadic amyotrophic lateral sclerosis patients." Brain Res **917**(1): 97-104.

Song, J. W., T. Misgeld, H. Kang, S. Knecht, J. Lu, Y. Cao, S. L. Cotman, D. L. Bishop and J. W. Lichtman (2008). "Lysosomal activity associated with developmental axon pruning." J Neurosci **28**(36): 8993-9001.

Spreux-Varoquaux, O., G. Bensimon, L. Lacomblez, F. Salachas, P. F. Pradat, N. Le Forestier, A. Marouan, M. Dib and V. Meininger (2002). "Glutamate levels in cerebrospinal fluid in amyotrophic lateral sclerosis: a reappraisal using a new HPLC method with coulometric detection in a large cohort of patients." J Neurol Sci **193**(2): 73-78.

Takeuchi, H., Y. Kobayashi, S. Ishigaki, M. Doyu and G. Sobue (2002). "Mitochondrial localization of mutant superoxide dismutase 1 triggers caspase-dependent cell death in a cellular model of familial amyotrophic lateral sclerosis." J Biol Chem **277**(52): 50966-50972.

Tradewell, M. L., L. A. Cooper, S. Minotti and H. D. Durham (2011). "Calcium dysregulation, mitochondrial pathology and protein aggregation in a culture model of amyotrophic lateral sclerosis: mechanistic relationship and differential sensitivity to intervention." Neurobiol Dis **42**(3): 265-275.

Trotti, D., A. Rolfs, N. C. Danbolt, R. H. Brown, Jr. and M. A. Hediger (1999). "SOD1 mutants linked to amyotrophic lateral sclerosis selectively inactivate a glial glutamate transporter." Nat Neurosci **2**(9): 848.

Turney, S. G. and J. W. Lichtman (2012). "Reversing the outcome of synapse elimination at developing neuromuscular junctions in vivo: evidence for synaptic competition and its mechanism." PLoS Biol **10**(6): e1001352.

Vale, R. D., B. J. Schnapp, T. S. Reese and M. P. Sheetz (1985). "Organelle, bead, and microtubule translocations promoted by soluble factors from the squid giant axon." Cell **40**(3): 559-569.

Vande Velde, C., M. L. Garcia, X. Yin, B. D. Trapp and D. W. Cleveland (2004). "The neuroprotective factor Wlds does not attenuate mutant SOD1-mediated motor neuron disease." Neuromolecular Med **5**(3): 193-203.

Vande Velde, C., K. K. McDonald, Y. Boukhedimi, M. McAlonis-Downes, C. S. Lobsiger, S. Bel Hadj, A. Zandona, J. P. Julien, S. B. Shah and D. W. Cleveland (2011). "Misfolded SOD1 associated with motor neuron mitochondria alters mitochondrial shape and distribution prior to clinical onset." PLoS One **6**(7): e22031.

Vande Velde, C., T. M. Miller, N. R. Cashman and D. W. Cleveland (2008). "Selective association of misfolded ALS-linked mutant SOD1 with the cytoplasmic face of mitochondria." Proc Natl Acad Sci U S A **105**(10): 4022-4027.

Walsh, M. K. and J. W. Lichtman (2003). "In vivo time-lapse imaging of synaptic takeover associated with naturally occurring synapse elimination." Neuron **37**(1): 67-73.

Wang, J. T., Z. A. Medress and B. A. Barres (2012). "Axon degeneration: molecular mechanisms of a self-destruction pathway." J Cell Biol **196**(1): 7-18.

Wang, X. and T. L. Schwarz (2009). "The mechanism of Ca2+ -dependent regulation of kinesin-mediated mitochondrial motility." Cell **136**(1): 163-174.

Warita, H., Y. Itoyama and K. Abe (1999). "Selective impairment of fast anterograde axonal transport in the peripheral nerves of asymptomatic transgenic mice with a G93A mutant SOD1 gene." Brain Res **819**(1-2): 120-131.

Watanabe, M., M. Dykes-Hoberg, V. C. Culotta, D. L. Price, P. C. Wong and J. D. Rothstein (2001). "Histological evidence of protein aggregation in mutant SOD1 transgenic mice and in amyotrophic lateral sclerosis neural tissues." Neurobiol Dis **8**(6): 933-941.

Wegorzewska, I., S. Bell, N. J. Cairns, T. M. Miller and R. H. Baloh (2009). "TDP-43 mutant transgenic mice develop features of ALS and frontotemporal lobar degeneration." Proc Natl Acad Sci U S A **106**(44): 18809-18814.

Wijesekera, L. C. and P. N. Leigh (2009). "Amyotrophic lateral sclerosis." Orphanet J Rare Dis **4**: 3.

Williams, D. W. and J. W. Truman (2005). "Cellular mechanisms of dendrite pruning in Drosophila: insights from in vivo time-lapse of remodeling dendritic arborizing sensory neurons." Development **132**(16): 3631-3642.

Williamson, T. L., L. I. Bruijn, Q. Zhu, K. L. Anderson, S. D. Anderson, J. P. Julien and D. W. Cleveland (1998). "Absence of neurofilaments reduces the selective vulnerability of motor neurons and slows disease caused by a familial amyotrophic lateral sclerosis-linked superoxide dismutase 1 mutant." Proc Natl Acad Sci U S A **95**(16): 9631-9636.

Williamson, T. L. and D. W. Cleveland (1999). "Slowing of axonal transport is a very early event in the toxicity of ALS-linked SOD1 mutants to motor neurons." Nat Neurosci **2**(1): 50-56.

Wils, H., G. Kleinberger, J. Janssens, S. Pereson, G. Joris, I. Cuijt, V. Smits, C. Ceuterick-de Groote, C. Van Broeckhoven and S. Kumar-Singh (2010). "TDP-43 transgenic mice develop spastic paralysis and neuronal inclusions characteristic of ALS and frontotemporal lobar degeneration." Proc Natl Acad Sci U S A **107**(8): 3858-3863.

Wong, P. C., C. A. Pardo, D. R. Borchelt, M. K. Lee, N. G. Copeland, N. A. Jenkins, S. S. Sisodia, D. W. Cleveland and D. L. Price (1995). "An adverse property of a familial ALS-linked SOD1 mutation causes motor neuron disease characterized by vacuolar degeneration of mitochondria." Neuron **14**(6): 1105-1116.

Wyatt, R. M. and R. J. Balice-Gordon (2003). "Activity-dependent elimination of neuromuscular synapses." J Neurocytol **32**(5-8): 777-794.

Zhang, B., P. Tu, F. Abtahian, J. Q. Trojanowski and V. M. Lee (1997). "Neurofilaments and orthograde transport are reduced in ventral root axons of transgenic mice that express human SOD1 with a G93A mutation." J Cell Biol **139**(5): 1307-1315.

Zhang, F., A. L. Strom, K. Fukada, S. Lee, L. J. Hayward and H. Zhu (2007). "Interaction between familial amyotrophic lateral sclerosis (ALS)-linked SOD1 mutants and the dynein complex." J Biol Chem **282**(22): 16691-16699.

Zhu, Y. B. and Z. H. Sheng (2011). "Increased axonal mitochondrial mobility does not slow amyotrophic lateral sclerosis (ALS)-like disease in mutant SOD1 mice." J Biol Chem **286**(26): 23432-23440.

Publications

Kerschensteiner, M., M. S. Reuter, et al. (2008). "Ex vivo imaging of motor axon dynamics in murine triangularis sterni explants." Nat Protoc **3**(10): 1645-1653.

Marinkovic, P., M. S. Reuter, et al. (2012). "Axonal transport deficits and degeneration can evolve independently in mouse models of amyotrophic lateral sclerosis." Proc Natl Acad Sci USA **109**(11): 4296-4301.

Brill, M., T. Kleele, M. S. Reuter & T. Misgeld. Branch-specific axonal transport deficits and microtubule destabilization during neuromuscular synapse elimination. In preparation

Data presentation

Molecular and Cellular Mechanisms of Axon Degeneration, Marine Biological Laboratory, Woods Hole, MA, USA, Oct 26th-28th, 2008 (Poster presentation)

Acknowledgements

I thank my supervisor Thomas Misgeld for the excellent mentoring and support during the compilation of my thesis. Through his valuable advice and discussions during my work in the lab I learned a lot and developed interest in scientific questions. I had much fun working in his lab, also due to the cordial and collaborative atmosphere among the colleagues. Thomas also supported me in other areas of my studies. I want to thank for his recommendations regarding the scholarships of the 'International Research Training Group 1373' and the 'Studienstiftung des deutschen Volkes', and the opportunity to present my data at an international conference in the USA. I also thank Leanne Godinho for the nice time and her support.

I want to thank our collaborators Martin Kerschensteiner and Florence Bareyre for the discussions and advice related to our projects.

A lot of thanks go to my colleague Petar Marinkovic for the great cooperation and the completion of our project, and particularly for the cheerful time. Thanks to my other colleagues Monika Brill, Tatjana Kleele, Peter Engerer, Barbara Plomer, Michael Breckwoldt, Ivana Nikic and Claudia Lang for the cooperation and the nice time with all of you.

I want to thank Manuela Budak, Yvonne Hufnagel, Anna Thomer and Rosi Karl for excellent technical assistance.

Special thanks go to my family, foremost my parents and my two sisters, who are always there for me and supported me during the compilation of my thesis and during my studies. Thanks to my mother for helping me with the statistical analyses. I thank Stefan for always being there for me.

I thank the 'International Research Training Group 1373' for financial support during my work in the lab.